

The background of the cover is an aerial photograph of a large body of water, likely Cook Inlet, completely covered in a thick layer of sea ice. The ice is broken up into numerous irregular, interconnected floes of varying sizes. In the upper portion of the image, a large, rugged mountain range is visible, its peaks and ridges heavily covered in snow and partially obscured by a light, hazy atmosphere. The overall color palette is dominated by various shades of blue, white, and light grey, creating a cold and desolate atmosphere.

Marine Ice Atlas for Cook Inlet, Alaska

**NATHAN D. MULHERIN
WALTER B. TUCKER III
ORSON P. SMITH
WILLIAM J. LEE**

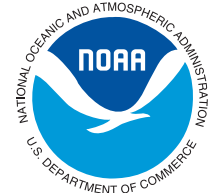
COVER: On a clear day in February, Mt. Iliamna is seen beyond close pack ice in Lower Cook Inlet. The ice cover is young, grey-white ice, first-year thin pancakes, and small floes of 7 to 8 tenths concentration. (Photo by Orson Smith)

May 2001

This atlas and other products of the Cold Regions Research and Engineering Laboratory are available through CRREL's web site: <http://www.crrel.usace.army.mil>



**US Army Corps
of Engineers®**
Engineer Research and
Development Center



**National Oceanic
and Atmospheric
Administration**
National Ocean Service

Marine Ice Atlas for Cook Inlet, Alaska

**NATHAN D. MULHERIN
WALTER B. TUCKER III
ORSON P. SMITH
WILLIAM J. LEE**

Prepared by

U.S. Army Corps of Engineers
Engineer Research and Development Center
Cold Regions Research and Engineering
Laboratory
ERDC/CRREL TR-01-10

Sponsored by

U.S. Department of Commerce
National Oceanic and Atmospheric
Administration
National Ocean Service
Office of Response and Restoration

PREFACE

This report was prepared by Nathan D. Mulherin, Research Physical Scientist, and Walter B. Tucker III, Geophysicist, Snow and Ice Division, U.S. Army Engineer Research and Development Center, Cold Regions Research and Engineering Laboratory (CRREL), Hanover, New Hampshire; and Dr. Orson P. Smith, Associate Professor, and William J. Lee, Research Analyst, School of Engineering, University of Alaska Anchorage (UAA). The publication was a product of the Cook Inlet and Prince William Sound Navigation Safety and Efficiency Project and was funded by the National Oceanic and Atmospheric Administration, National Ocean Service, Office of Response and Restoration.

The authors are grateful to Dr. Andrey Proshutinsky, Arctic Chair in Marine Science at the Naval Postgraduate School, and to Craig Evanego, Ice Analyst at the National Naval Ice Center, for their technical reviews of the manuscript. Grateful acknowledgment is also extended to the World Meteorological Organization, Geneva, Switzerland, for permission to use their sea ice nomenclature (WMO 1970), which appears here as Appendix A; to Russell Page, Meteorologist and Ice Analyst, National Weather Service Forecast Office in Anchorage, Alaska, for helpful discussions concerning Cook Inlet ice analysis and forecasting; and to Dwight Pollard, State Climatologist, Alaska State Climate Center, Anchorage, Alaska, for assisting in the retrieval of archived NWS ice maps. They also thank MSgt John Johnson, Analyst, and Capt. Gary Marsteller, Assistant Chief of the Climatological Applications Team 2, Air Force Combat Climatology Center, Asheville, North Carolina, for compiling and summarizing the climatological data.

Many other individuals at CRREL and UAA were instrumental in producing this report. Those at CRREL include Paul Cedefeldt, Physical Scientist, Geochemical Sciences Division, for providing advice and assistance in formulating our geographic information database; Brian Tracy, Physical Scientist, Remote Sensing/GIS Center, for accessing satellite images; Jane Mason and Dawn Boden for figure preparation; David Cate for editing; and John Severance for final production. Melanie Hartman and Cathy Huot at UAA assisted in compiling the GIS database from the NWS ice charts.

The contents of this report are not to be used for advertising or promotional purposes. Citation of brand names does not constitute an official endorsement or approval of the use of such commercial products.

CONTENTS

Preface	i
Abbreviations and conversions	vi
1 Introduction	1
2 Cook Inlet Physical Description	3
2.1 Regional geography	3
2.2 Cook Inlet's Head region	3
2.3 Upper Cook Inlet	6
2.4 Lower Cook Inlet	6
3 Cook Inlet Marine Ice	9
3.1 Ice types	9
3.2 General marine ice environment	13
3.3 Theoretical ice growth and melt	17
3.4 Cook Inlet marine ice data	18
4 Expected Ice Conditions	25
Map Set 1. Mean ice concentration and stage of development	26
Map Set 2. Probability of occurrence for ice of any stage of development and ice of any concentration	35
Map Set 3. Probability of occurrence for ice of any stage of development and ice of at least 5/10ths concentration	44
5 Oceanography	53
5.1 Bathymetry	53
5.2 Currents and tides	53
6 Climatology	59
6.1 Source and description of climatological data for Cook Inlet	59
6.2 Station climatologies	61
6.3 Duration of daylight	71

7 Literature Cited	75
Appendix A: Sea Ice Nomenclature, Arranged by Subject	79
Appendix B: Example of a Cook Inlet Ice Cover Analysis Issued by the National Ice Center in Suitland, Maryland	87
Appendix C: Procedure Used to Create the Composite Cook Inlet Ice Charts	91
Appendix D: Air Temperature	95
Appendix E: Wind	109
Appendix F: Wind Chill	123
Appendix G: Sea Level Pressure	125
Appendix H: Bibliography	139

ILLUSTRATIONS

Figure 1. Cook Inlet and relief map of surrounding region	4
Figure 2. Place names of the Head Region of Cook Inlet	5
Figure 3. Young, gray, and gray-white ice, some floes white with snow cover, moving with the tide past the Port of Anchorage in Lower Knik Arm	5
Figure 4. Place names of Upper Cook Inlet	6
Figure 5. Place names of Lower Cook Inlet	7
Figure 6. Brash ice clogging Homer's small boat harbor to an unusual extent	8
Figure 7. Relationship between the temperature of maximum density and the freezing point of water with respect to salinity	10
Figure 8. Relationship between the thickness of young sea ice, accumu- lated freezing degree-days, and snow cover thickness	10
Figure 9. Typical mixed-ice conditions in Upper Cook Inlet, featuring ice floes, both level ice and shove-thickened pans, interspersed with broken and brash ice in various first-year thin stages of development	14
Figure 10. Dates of significant ice formation at the Phillips Platform with respect to freezing degree-days	16
Figure 11. Mean monthly freezing and thawing degree-days for 1974– 1997 assuming base temperatures of 0 and -1.8°C , respectively, for four locations on Cook Inlet	20
Figure 12. Seasonal variation of freezing and thawing degree-days for 1974–1997 for four locations on Cook Inlet	21
Figure 13. Season total FDDs for Anchorage, Alaska	21
Figure 14. Radarsat-1 SAR imagery showing the Forelands area of Cook Inlet at near low tide on December 30, 1998	23
Figure 15. Example of a sea ice analysis chart issued by the Alaska Region Headquarters of the National Weather Service	24
Figure 16. Cook Inlet bathymetry	54

Figure 17. Tidal mudflats in Upper Cook Inlet and the Head Region	54
Figure 18. General surface circulation pattern in Cook Inlet	55
Figure 19. Summer surface circulation pattern in Lower Cook Inlet	56
Figure 20. Tidal ranges at various locations around Cook Inlet	57
Figure 21. Alaska's climatic zones	60
Figure 22. Weather summary for Anchorage International Airport	62
Figure 23. Average percent possible sunshine at Anchorage International Airport from 1955 to 1993	63
Figure 24. Weather summary for Kenai Municipal Airport	65
Figure 25. Weather summary for Homer Municipal Airport	67
Figure 26. Weather summary for Kodiak Municipal Airport	69
Figure 27. Median monthly precipitation from 1961 to 1990 for four Cook Inlet locations	70
Figure 28. Total length of daylight for Alaska locations	71

TABLES

Table 1. Vessel and structure damage in Cook Inlet caused by floating ice	11
Table 2. Dates of river ice break-up and freeze-up	13
Table 3. Dates of first significant ice and ice-out for northern Cook Inlet ...	15
Table 4. Dates of first significant ice for Upper and Lower Cook Inlet, and corresponding freezing degree-days at Anchorage and Kenai, respectively	16
Table 5. Ice design criteria for Cook Inlet petroleum industry platforms	17
Table 6. Accumulated freezing and thawing degree-days at Anchorage, Alaska, and calculated sea ice growth and melt in Cook Inlet	19
Table 7. Stream flow data for the Matanuska, Knik, and Susitna Rivers	55
Table 8. Location and description of first-order Cook Inlet meteorological stations used in this study	60
Table 9. Local times of sunrise and sunset at Kenai, Alaska, for the year 2000	72

ABBREVIATIONS

ACRC	Alaska Climate Research Center
AEIDC	Alaska Environmental Information and Data Center
AFCCC	Air Force Combat Climatology Center
API	American Petroleum Institute
asl	above sea level
AVHRR	Advanced very high resolution radiometer
DMSP OLS	Defense Meteorological Satellite Program Operational Linescan System
FDD	freezing degree-day
GIS	Geographic information system
MLLW	mean low low water
NCDC	National Climatic Data Center
NCEP	National Centers for Environmental Prediction
NIC	National Ice Center
NOS	National Ocean Service
NWS	National Weather Service
POR	period of record
ppt	parts per thousand
SAR	Synthetic aperture radar
SSM/I	Special sensor microwave/imager
TDD	thawing degree-day
USACE	U.S. Army Corps of Engineers
USCB	U.S. Census Bureau
USCG	U.S. Coast Guard
USNO	U.S. Naval Observatory
WMO	World Meteorological Organization

CONVERSIONS

Distance

3.28084 ft = 1 m

0.53996 nautical miles = 1 km

0.62137 U.S. statute miles = 1 km

Velocity

0.86898 knots = 1 mph

1.94385 knots = 1 m/s

0.62137 U.S. statute miles/hr = 1 km/hr

0.44704 m/s = 1 U.S. statute miles/hr

1.1508 U.S. statute miles = 1 nautical mile

0.53995 knots = 1 km/hr

Flow volume

0.02832 m³/s = 1 cfs

1 INTRODUCTION

Cook Inlet is a 350-km-long estuary located in south-central Alaska. Approximately half the population of Alaska resides near its shores. Anchorage, situated near its northern end, is the state's largest city and a major center for commerce, industry, recreation, and transportation. Shipping routes in Cook Inlet serve year-round oil and natural gas production in central Cook Inlet and the import of consumer goods and petroleum products to the Port of Anchorage. The Port serves 80% of Alaska's population and its four largest military bases.

The marine ice environment of Cook Inlet is unique. Tidal height variations at Anchorage are the second most extreme in the world. At 9 m, they are exceeded only by those that occur in eastern Canada's Bay of Fundy. The extreme tidal range and the generally shallow nature of Cook Inlet produce extreme tidal currents as well. Tidal currents at maximum flow are typically 4 knots and have been reported to be as high as 8 knots. These bathymetric and oceanographic factors, in combination with the winter climate, result in the production of large quantities of marine ice in Cook Inlet that can impact human activities for substantial periods each year.

A report by Gatto, published in 1976, was the most comprehensive information publicly available up to that time on the oceanography of Cook Inlet. A section of that report was devoted to the Inlet's sea ice environment. However, it wasn't until 1983, when the Alaska Marine Ice Atlas (LaBelle et al.) appeared, that a time series of maps became available that depicted

the sea ice extent and character for Cook Inlet in particular. The maps were based on a large array of published and unpublished sources and the several intermittent ice maps that had been issued by the National Weather Service (NWS). Shortly thereafter the NWS began to regularly issue Cook Inlet ice charts showing the current conditions as an aid to navigation and fishing activities. As of April 1999, approximately 675 such charts had been archived and are now available for analysis. One purpose of this publication is to present an updated time series of the mean and extreme sea ice conditions that we derived from these charts. In addition, this report is a compilation of previously published and unpublished information on the severity of winter conditions that prevail in a region important for the nation's commercial activities. The information contained here is intended to aid engineers, ship owners, port and government officials, planning agencies, and mariners in ship design and modification criteria; in planning safe and efficient navigation in Cook Inlet; and in regional development decision-making and contingency planning.

Section 2 of this atlas provides a physical description of Cook Inlet and the surrounding region. Section 3 describes the Inlet's marine ice environment. Section 4 contains the maps of Cook Inlet ice cover that we created from a quantitative analysis of the NWS ice charts. Sections 5 and 6 describe the oceanographic and climatic factors, respectively, that contribute to the ice regime of Cook Inlet.

2 COOK INLET PHYSICAL DESCRIPTION

2.1 Regional geography

Cook Inlet is oriented southwest-northeast and centered at approximately 60°N latitude and 152°W longitude (Fig. 1). The land surrounding Cook Inlet consists of vast tidal marshlands, rising up to piedmont lowlands with many lakes and ponds, to rugged glacially carved mountains. Estuarine tidal marshes are prevalent at the mouths of the rivers and as large portions of the bays about the Inlet. The Kenai Peninsula encloses Cook Inlet to the southeast. Here, the Kenai Lowlands, immediately adjacent to the Inlet, is an area of flat marshland, lakes, and bogs that gradually rises up to rolling piedmont foothills. These lowlands and foothills extend over a distance of 50–65 km eastward to the Kenai Mountains, which rise to approximately 1,500 m (5,000 ft) above sea level (asl).

Immediately east of the state's largest city, Anchorage, are the Chugach Mountains, which rise abruptly to around 2,150 m (7,000 ft) asl. The climate of the Chugach Range is strongly influenced by its close proximity to the Gulf of Alaska. The cold, polar air masses that sweep down across Alaska's interior and collide with the Gulf's warmer, moisture-laden air produce over 15 m of snowfall annually.

The Talkeetna Range, northeast of the Inlet, is separated from the Chugach Mountains to the south by the Matanuska River valley and from the Alaska Range to the north by the Susitna River. The Talkeetnas reach 2,150 m (7,000 ft) in elevation. The Alaska Range contains several of the highest peaks in North America, including Denali (or Mt. McKinley – 6,194 m [20,320 ft]) and Mt. Foraker (5,304 m [17,400 ft]). However, aside from the several giants (fewer than 20 peaks in the range are taller than 3,000 m), these mountains are generally 2,150–2,750 m (7,000–9,000 ft) high.

Curving around to the northwest of the Inlet, the

Alaska Range blends almost imperceptibly with the Aleutian Range, which continues along the Lower Inlet's western edge, with summits averaging 1,525 m (5,000 ft) in elevation. However, many of the Aleutian Mountains are much taller and are active volcanoes. Of these, and within sight of Cook Inlet, are Mounts Spurr (3,374 m [11,070 ft]), Redoubt (3,108 m [10,197 ft]), Iliamna (3,053 m [10,016 ft]), and Douglas (2,153 m [7,064 ft]). Mount Augustine is a 4,025-m [13,205-ft] volcano that rises abruptly out of the waters of the Lower Inlet as Augustine Island.

Extending north from Cook Inlet and enclosed by the Talkeetna and Alaska Ranges are the Susitna Lowlands. They are a poorly drained, glaciated basin, approximately 145 km long and 130 km wide, that is characterized by its extensive ground moraine, outwash plains, drumlin fields, eskers, kettles, and swampland.

2.2 Cook Inlet's Head region

Cook Inlet can be described as three distinct regions (the Head, the Upper Inlet, and the Lower Inlet) (Nelson 1995). The Head, or northernmost end of the Inlet, is composed of two long and narrow bays known as Knik and Turnagain Arms (Fig. 2). Knik Arm extends inland approximately 50 km to the confluence of the Knik and Matanuska Rivers from a line connecting Points Woronzof and MacKenzie. It ranges from 2 to 10 km wide over its length. The upper two thirds is almost entirely exposed mudflats during low tide. The Port of Anchorage is located at the mouth of Ship Creek on the southeast shore of Knik Arm, approximately 7 km northeast of Point Woronzof and 280 km from the Gulf of Alaska. Anchorage (with a population estimated at 255,000 in 1998) is nearly eight times larger than the state's second largest city

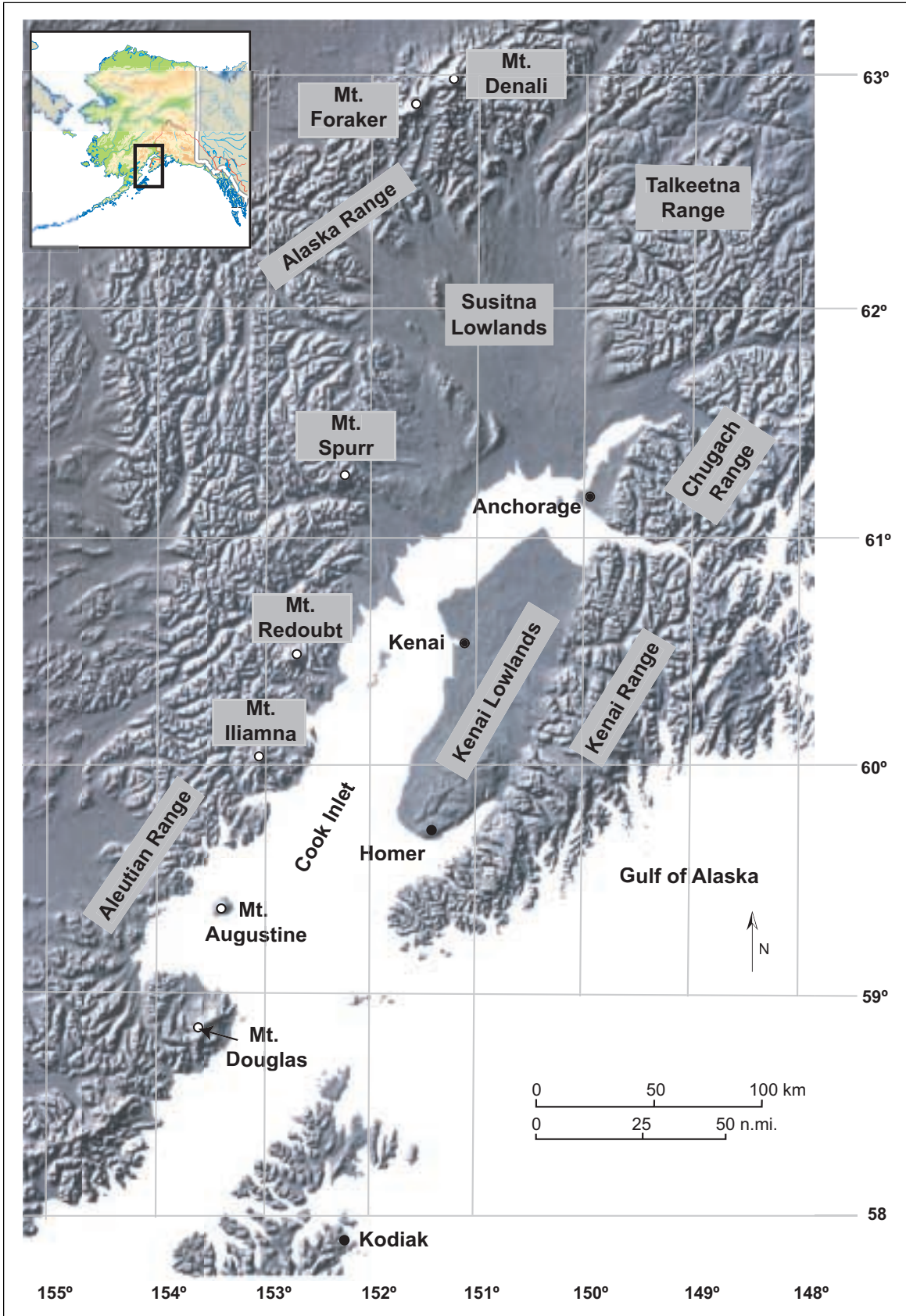


Figure 1. Cook Inlet and relief map of surrounding region.

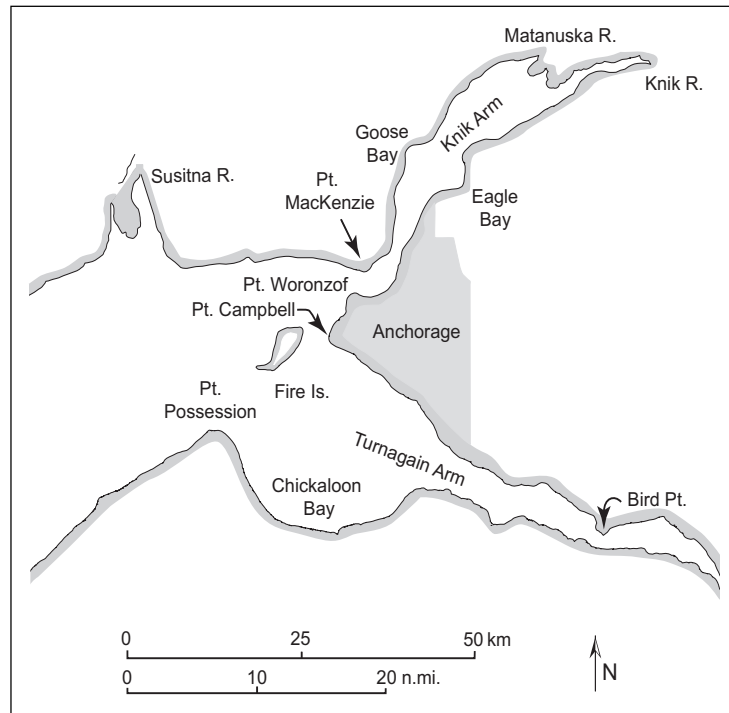


Figure 2. Place names of the Head Region of Cook Inlet.



Figure 3. Young, gray, and gray-white ice, some floes white with snow cover, moving with the tide past the Port of Anchorage in Lower Knik Arm. (Photo by Orson Smith.)

of Fairbanks (USCB 1999). The port has one deep-draft wharf with berthing space for three vessels, a petroleum terminal dock, several docking wharves for barges, and a small-boat marina (Fig. 3).

Turnagain Arm extends approximately 75 km eastward from a line between Point Campbell and Point Possession to the railroad depot at Portage and varies from 2 to 26 km in width. It, too, exhibits extensive tidal mud flats during low water. Fire Island is located at the dividing point of Knik and Turnagain Arms, 5 km west of Point Campbell.

2.3 Upper Cook Inlet

Upper Cook Inlet, approximately 95 km long, lies between Point Campbell and the East and West Forelands (Fig. 4). The Forelands are opposing peninsulas that constrict the Inlet to about 16 km in width, whereas the Upper Inlet typically ranges from 20 to 30 km wide. The shoreline is very regular, with few coves and inlets. This section's largest bay, Trading Bay, occupies the area between West Foreland and Granite Point. Smaller bays include Beshta Bay (north of Granite Point) and Nikiski Bay (north of East

Foreland). The major rivers that enter the Upper Inlet are the Susitna and Little Susitna, the Beluga, and the McArthur, all of which drain out of the Alaska and Talkeetna mountain ranges and discharge into Cook Inlet from the north.

Several shoals are present in this region, including Middle Ground Shoal, just north of the Forelands, lying parallel to and just north of the Inlet's midline, and Beluga Shoal at midline and due south of the Susitna River's mouth. Fire Island Shoal, which lies due west of Fire Island; North Point Shoal; and Knik Arm Shoal all challenge navigation into and out of Knik Arm and the Port of Anchorage.

2.4 Lower Cook Inlet

The largest region, Lower Cook Inlet (Fig. 5), extends 200 km southwest beyond the Forelands to its mouth, which opens into the Gulf of Alaska. The mouth is located between Cape Douglas on the Alaska Peninsula and Cape Elizabeth on the Kenai Peninsula side. There are three entrances from the Gulf of Alaska into Cook Inlet. These are, from east to west, Kennedy Entrance and Stevenson Entrance, which are separated by the Barren Islands, and Shelikof Strait, which sepa-

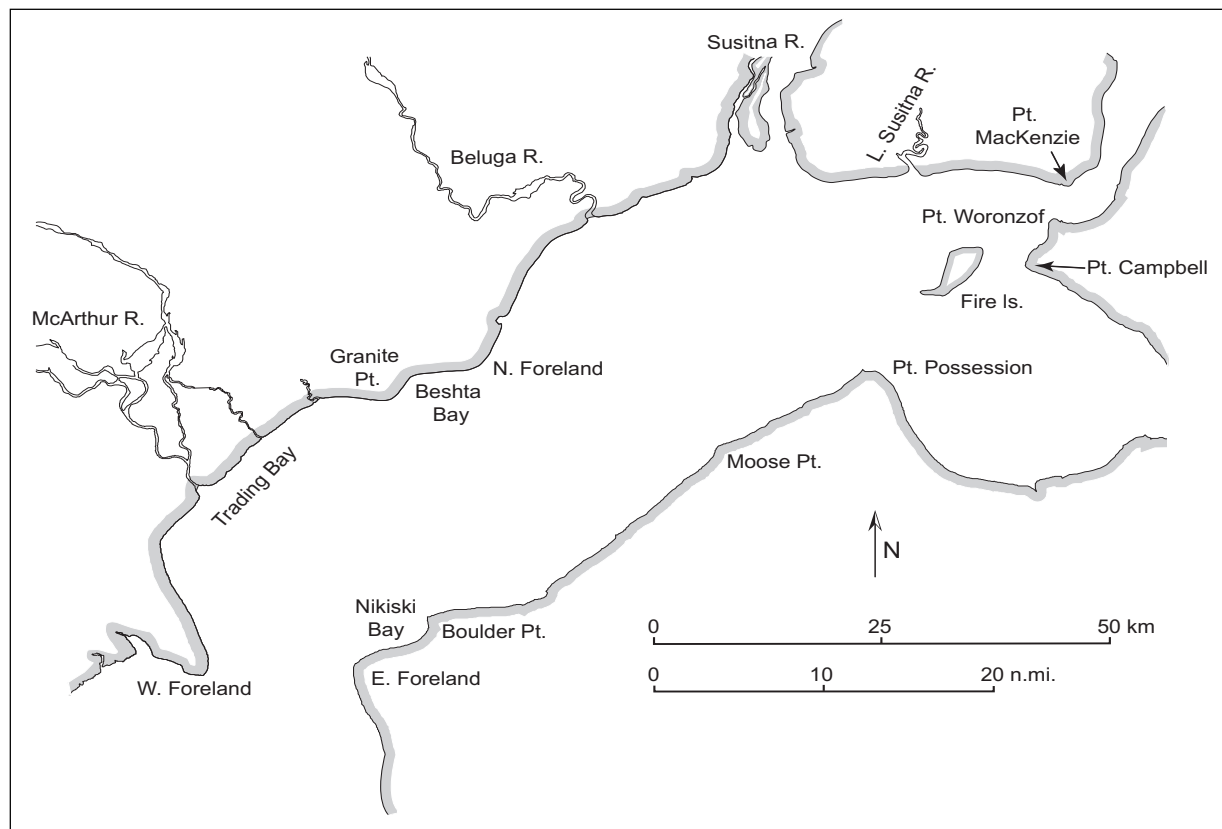


Figure 4. Place names of Upper Cook Inlet.

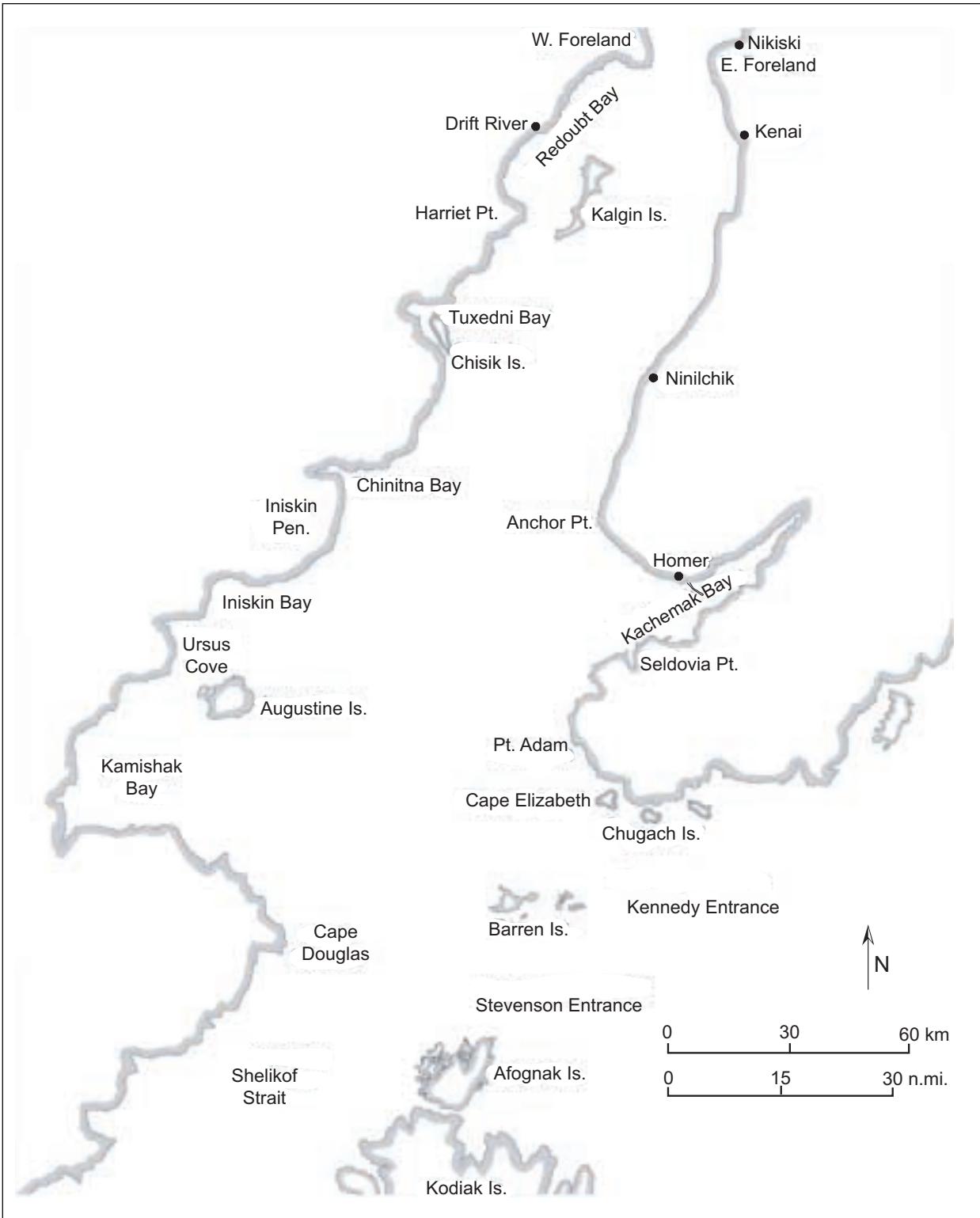


Figure 5. Place names of Lower Cook Inlet.



Figure 6. Brash ice clogging Homer's small boat harbor to an unusual extent. (Photo by Orson Smith.)

rates Kodiak and Afognak Islands from the Alaska Peninsula. The eastern shoreline north of Homer and the western shoreline north of Harriet Point border on lowland outwash plains, with mountains that are distant from the coast. As such, there is little undulation and few sheltering coves along these shorelines, with the exception of Redoubt Bay, between West Foreland and Harriet Point. However, south of those points, the shorelines are more mountainous and indented with numerous bays, inlets, and coves. Other major bays of the Lower Inlet include Kachemak, Kamishak, Tuxedni, Chinitna, and Iniskin Bays, and Ursus Cove. With the exception of Kachemak Bay, all are located along the western shoreline.

The largest two bays, Kachemak and Kamishak, are located on opposite shores at the southern end of Lower Cook Inlet. Kachemak Bay is 35 km wide at its mouth between Seldovia Point and Anchor Point. It reaches about 40 km inland, tapering gradually to 4 km wide where it ends at the mouth of the Fox River. Its northern shoreline, the southern terminus of the Kenai Lowland, is regular and non-undulating. Its southern shoreline, however, abuts the spine of the Kenai Mountains and is punctuated with many long

finger fiords and small bays. Homer Spit, jutting south-eastward into the bay from the town of Homer, is founded on a glacial deposit nearly 8 km long and less than a half kilometer wide, creating a natural breakwater and excellent anchorage for the large commercial fishing fleet based there. Homer, also a center for tourism, has a population of about 4,800. Marine facilities there include a deep-water dock that can accommodate two 340-ft-long vessels with 30-ft or less draft, a 740-vessel-capacity small-boat harbor (Fig. 6), an Alaska Marine Highway System terminal, a U.S. Coast Guard station, and storage and shipment facilities for fish, petroleum products, and general cargo.

On the western side of Cook Inlet is Kamishak Bay. It is approximately 33 km long from its 43-km-wide entrance between Douglas Reef and Tignavik Point.

There are several large islands situated within the Lower Inlet. These include Augustine Island, in Kamishak Bay, and Chisik Island, at the mouth of the Tuxedni Bay. Kalgin Island, about 30 km south of the Forelands, plays an important role in the permanent and tidal currents that dominate the hydrodynamic regime of the Inlet. The Barren Islands and Chugach Islands are located at the Inlet's mouth.

3 COOK INLET MARINE ICE

3.1 Ice types

The ice types that form in Cook Inlet are described in Brower et al. (1988) as

- Sea ice,
- Beach ice,
- Stamukhi, and
- Estuarine and river ice.

Nelson (1995) categorized the ice types as

- Floating ice forming under non-turbulent water and air conditions,
- Floating ice forming under turbulent conditions, and
- Shorefast ice,

each dependent on the ambient air temperature, wind conditions, water salinity, and tide and turbulence levels at the time of formation. Here, we distinguish between the types of Cook Inlet ice using the terms

- Pack ice,
- Shorefast ice,
- Stamukhi, and
- Estuarine and river ice.

In reality, sea ice often forms as some combination of these types but usually can be classified as more of one type than others. The World Meteorological Organization's nomenclature of sea ice, which is useful for further clarification of terminology, is included as Appendix A.

3.1.1 Pack ice

The term "pack ice" can be used to denote any form

of freely floating sea ice forming directly from the freezing of seawater. Its formation sequence is as follows. Water contracts as it cools, until it reaches 4.0°C, the temperature of maximum density for fresh water. With further cooling, water expands continuously until it freezes at 0°C. Adding salt not only lowers the freezing point of water but also lowers its temperature of maximum density. Figure 7 shows the relationship between salinity and the temperatures of maximum density and freezing. At 24.7 parts per thousand (ppt) salt, the two lines converge, indicating that water of even greater salinity will freeze at its point of maximum density. Typical seawater has a salinity of about 35 ppt and freezes at -1.9°C.

As the temperature of seawater near the surface decreases, a vertical density gradient forms in the water column. The colder and heavier seawater sinks, while warmer, less dense seawater from below rises to take its place. Ideally the density gradient disappears when the entire water column becomes uniformly cooled to its freezing point. However, the seas do not have uniform top-to-bottom salinity. Instead, there exists a density boundary between the surface and the deeper waters, known as the "halocline," across which vertical mixing does not occur, in the absence of other forces. The deeper water is warmer, but its higher salinity prevents it from rising to mix with the chilled surface water. The effect is that the ocean surface can freeze when the surface layer alone has attained its freezing point, even though there may be considerable heat trapped below the halocline.

In the absence of turbulence, ice crystals can form anywhere within this upper layer of water. The crystals float to the surface and form a skim, which consolidates and thickens progressively downward as more crystals form at the ice-water interface. Under

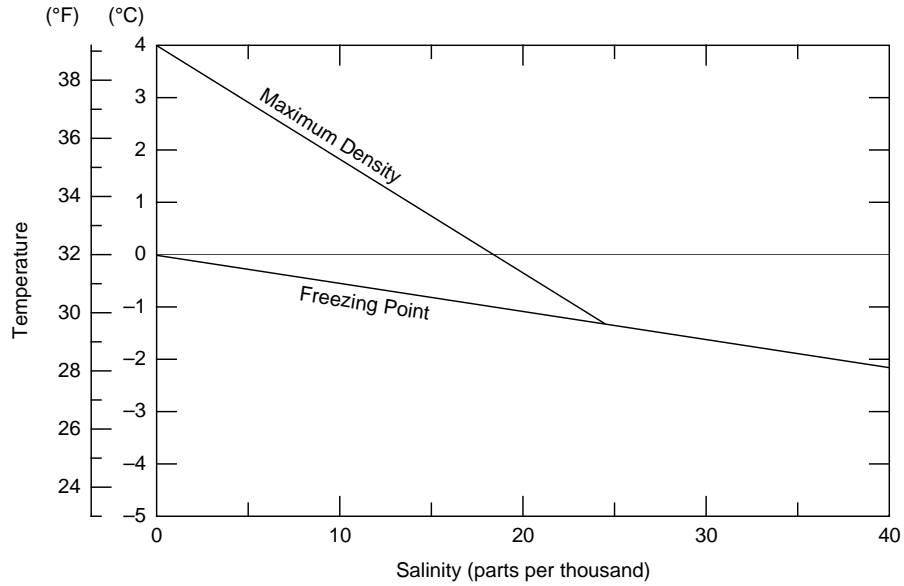


Figure 7. Relationship between the temperature of maximum density and the freezing point of water with respect to salinity. (After Bowditch 1977.)

conditions of low turbulence, the crystals on the bottom side of the ice cover grow downward, becoming elongated and columnar shaped. This process is known as congelation growth. The thickening ice cover becomes a barrier to heat flow between the water and the colder air above it. As the ice thickens, the loss of heat needed to maintain the ice growth process is slowed.

Snow on top of the ice cover acts as an even greater insulator, further decreasing the growth rate (Fig. 8). Despite snow's insulating effect, a thick snow cover can sometimes speed the process of ice thickening. When the snow weighs enough to depress the ice surface below the water level, hydrostatic pressure causes water to seep up through the ice and saturate the overlying snow. Air temperatures that are sufficiently cold

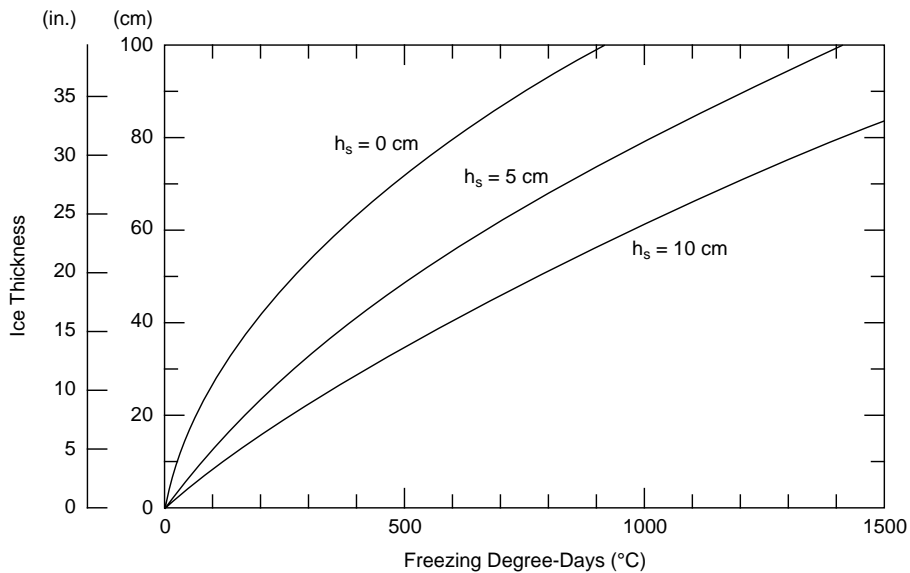


Figure 8. Relationship between the thickness of young sea ice, accumulated freezing degree-days, and snow cover thickness, h_s . (After Untersteiner 1986.)

will freeze the saturated snow from the top downward, creating a layer of “snow ice,” which will eventually bond to the sea ice if low temperatures persist. Nelson (1995) reported that snow ice comprises a large amount of the ice cover in Cook Inlet.

In the relatively shallow and highly turbulent waters of Cook Inlet, “frazil” ice is also a major component of the new ice that forms. Frazil is formed from tiny ice plates or needles that rapidly accumulate in turbulent water when colder water and air near the surface mix with warmer, deeper water. These ice crystals flocculate into low-density masses that float to the surface to form a soupy layer of unconsolidated ice, giving a greasy appearance to the water surface.

The next stage in the development of sea ice is “shuga”—ice crystals that continue to coalesce into floating pans and soon acquire a white, slushy appearance. Wind, wave, and current motion cause these pans to collide repeatedly, deforming and thickening their outer edges to create what is known as “pancake ice.” With further hardening, thickening, and consolidation, ice pans increase in size, sometimes forming larger floes or sheets of ice. Blenkarn (1970) reported that ice floes in the Inlet can be classified as “big” (greater than 500 m across [Appendix A]), with 400-m-wide floes being common. These floes and sheets some-

times collide, override one another, and freeze together to form ice that is immediately doubled in thickness. This process is known as “rafting.” Another type of consolidation and thickening, known as “fingering,” occurs when two pans merge and interlock such that the edges of one floe alternately slide over and under the adjacent floe.

Collision and stress between stronger and thicker ice sheets result in more extreme edge deformation, consolidation, and piling up of ice, known as “pressure ridging.” Depending on the magnitude and direction of the stresses, floating ice sheets (floes) can converge on other floes, fast ice, the shore, or the sea bottom and create large pressure ridges. In Cook Inlet, pressure ridges have been reported to be as thick as 6 m (Blenkarn 1970); no other quantitative information concerning ice thickening, roughness, or floe size and spacing is available.

Ice propelled by the tides presents the greatest danger to navigation and marine structures in Cook Inlet. Table 1 lists incidents that occurred between 1960 and 1986 from U.S. Coast Guard records of damage caused by floating ice.

More recently, problems caused by floating ice have been reported in the news. In February 1990, cargo loading of three oil tankers at Drift River Terminal

Table 1. Vessel and structure damage in Cook Inlet caused by floating ice. (After USCG 1991.)

<i>Date</i>	<i>Location</i>	<i>Damage</i>	<i>Cause of Accident</i>
11/29/64	Port of Anchorage	Pilings torn from petroleum dock, approx. \$33,000 damage	Winter ice and tides
12/12/64	Off port of Anchorage	Icebreaker <i>Milton II</i> caught in ice	Winter ice
3/29/67	Anchorage City Dock	Dock extension torn from pilings and demolished, \$1.9 million damage	Winter ice
5/2/67	Knik Arm Shoal	Tanker <i>Evje IV</i> ruptured cargo of oil tanks after striking shoal	Winter ice ripped out marker buoy
12/24/80	Port of Anchorage	540-ft SS <i>Philadelphia</i> struck underwater object, \$300,000 damage	Ice pan pushed ship into obstacle
2/24/82	Fire Island Shoal	497-ft SS <i>Newark</i> grounded	Heavy ice and tide
1/10/83	Port of Anchorage	523-ft SS <i>Galveston</i> came loose from dock when ice severed mooring lines, slight damage	Ice floe and tide
3/5/86	Anchorage City Dock	540-ft SS <i>Philadelphia</i> collided with dock, \$14,000 damage to 7 fender pilings	Large ice pan forced ship into dock

(on the western shore, across from Kenai) had to be suspended for a day due to heavy ice. Operators were forced to cast off and spend the night offshore, as it was feared that ice propelled by the tidal current would cause their vessels to be ruptured on the pier. The same news article mentioned a tanker-puncture incident in 1988 resulting in a small crude oil spill that was caused by similar conditions at the off-loading terminal at Nikiski (Kizzia 1990). Later that year, in December, Wohlforth (1990) wrote that heavy ice and currents stripped the MV *Coast Range* from the Drift River pier during loading operations, resulting in another spill estimated at 0.75–2.3 m³ (200–600 gallons). In February 1999, moving ice pushed the MV *Ocean Laurel* into Unocal's dock at Nikiski, causing \$100,000 in damage to the dock and catwalk (Associated Press 1999). A week later, heavy ice conditions in the Lower Inlet cracked a cargo storage tank aboard the MV *Chesapeake Trader* (Little 1999, ADEC 1999), allowing a spill of approximately 1.6 m³ (420 gallons). In January 2000, ice clogged the cooling-water intake of the freighter MV *Torm Pacific*, causing a brief loss of power and necessitating retreat to less troublesome waters until conditions improved (Little 2000a). A week later, two more vessels that were taking on urea and fuel were stripped from Tesoro's and Unocal's docks in Nikiski. One of the ship's pilots stated that the ice was "fairly soft but massive, about a foot and a half thick [0.5 m]... some of the pans are two miles in diameter [3200 m]." Approximately 0.75 m³ (200 gallons) of gasoline were spilled as tide-borne ice overwhelmed the mooring cables and tugboats that were attempting to hold them in place. The Coast Guard suspended cargo transfer there for several days until the ice conditions subsided (Little 2000b).

3.1.2 Shorefast ice

Ice that forms and remains firmly attached to the shoreline, stationary structures, or other nonmoving ice is known as "fast ice." It can form directly from freezing of the surrounding water, from piling and subsequent re-freezing of brash ice or broken ice of any age, or from flooding of snow atop shorefast ice.

Because of the large tidal range, extensive areas of mudflats around Cook Inlet are exposed to air temperatures low enough to freeze the upper layers of mud. With the flood tide, the seawater in contact with the frozen mud can freeze and bond to the bottom, forming beach ice. Successive low tides allow the stranded ice to attain ambient air temperature. When the air temperature is significantly lower than the seawater temperature, the ice can become progressively thicker with each succeeding high tide. As much as 2.5 cm (1 in.) of ice per tidal flood can accumulate in this manner,

but it will usually float free from the bottom before reaching about 0.5 m (1.6 ft) in thickness (Blenkarn 1970). At the point where buoyancy overcomes the bond strength, the ice lifts free and takes with it the topmost layer of sediment. This mechanism is the reason for much of the black coloration typical of the ice found in the Upper Inlet. The newly freed ice then either drifts into deeper water and continues growing or melting in the same manner as pack ice, or is floated higher on the beach, where it becomes stranded again and continues growing as "stamukha."

3.1.3 Stamukha

The term "stamukhi," the plural of stamukha, originated from the Russian ice classification and refers to sea ice that has broken and piled upward, or hummocked, because of wind, tides, or thermal expansion forces. Under certain conditions, massive ice blocks can form through

- Repeated wetting and accretion of seawater,
- Crushing and piling consolidation, or
- Stranding of successive layers of floating ice cakes on top of others, which, in turn, freeze together.

The term has appeared in numerous publications referring to the very largest ice cakes that are characteristic of Cook Inlet. Smith (2000) provided a detailed description of the stamukha formation process as beginning with the formation of beach ice. That is, incoming tide water forms thin, bottom-fast ice on cold-soaked mud flats. High tides deposit floating cakes and brash atop the bottom-fast ice, where they become stranded by the ebbing tide. Alternatively buoyancy may break loose some of the bottom-fast ice pieces so that they become stranded atop other sections of ice that are still adhered to the mud when the tide again recedes. The stacked pieces then freeze together and become increasingly stronger as a unified mass.

Stamukhi in Cook Inlet were reported by Nelson (1995) as thick as 7.5 m, and up to 12.2 m (40 ft) thick by Hutcheon (1972b) and Gatto (1976). Blenkarn (1970) described the typical stamukha as 4.6 m (15 ft) high and 6.1 m (20 ft) in diameter. Because of their large size, beached stamukhi are the last remnants of the ice cover to be seen in late spring. Tidal action occasionally will free stamukhi from the beach, floating them into deeper water where they can entrain with the pack ice. Because of their large mass and relative strength, drifting stamukhi are hazardous to shipping. In the brash ice conditions that are common in Cook Inlet, stamukhi are sometimes difficult to distinguish. They are, however, readily distinguishable among level ice floes because of their higher freeboard and irregu-

Table 2. Dates of river ice break-up and freeze-up. (After NOS 1994, p. T-21.)

Place	Waters	Ice Break-up			Ice Freeze-up			Years of Record
		Earliest	Average	Latest	Earliest	Average	Latest	
Susitna	Susitna River	4/12/41	May 1	5/10/46	10/19/33	Nov 1	11/14/36	1933-46
Kasilof	Kasilof River	3/27/41	Apr 13	4/29/46	11/13/45	Dec 3	12/24/48	1937-47
Kenai	Kenai River	3/18/52	Apr 2	4/14/51	11/23/51	Dec 10	12/26/37	1937-52
Anchorage	Ship Creek	2/16/44	Mar 29	4/17/42	11/10/35	Nov 24	12/10/36	1915-53

lar, sediment-laden sails. Smith (2000) reported that brine ice cores melted from stamukhi contained a mean salinity of only 1.07 ppt but a sediment concentration of 25 g/L, and more than 50% of the sediment particles by weight were greater than 63 μm in diameter (sand-sized).

3.1.4 Estuarine and river ice

A significant portion of Cook Inlet's ice is fresh-water ice that forms in the rivers and estuaries, especially in Knik and Turnagain Arms. Estuarine ice is similar in life cycle to sea ice, but it is significantly stronger and tends to remain more securely in place as fast ice. In the Upper Inlet, where the wind and water stresses are greater, estuarine ice is commonly entrained in the moving pack ice, where it is more of a danger to vessels and shoreline structures because of its strength. River ice is generally unaffected by the tides, wind, and waves, at least until spring break-up. At that time a considerable amount of river ice, pieces of which can sometimes be 2 m thick (Brower et al. 1988), is discharged into the Inlet. Table 2 shows spring break-up and fall freeze-up data for several rivers in the region.

3.2 General marine ice environment

The ice cover in Cook Inlet is seasonal, forming in the fall and disappearing completely each spring. Typically formation first occurs in October but does not cover a significantly large area until late November. By December about half the Inlet area north of the Forelands is normally covered with new ice and pancake ice (up to 10 cm thick) and thin, first-year ice (30–70 cm thick). Much of the ice cover is brash ice that has been broken by tidal movement and further thickened by compaction, fingering, rafting, hummocking, and ridging (Fig. 9). It ranges in concentration primarily from open (1/10, or 10% ice coverage for a given area) to close pack (7/10 to 8/10). The area south of the Forelands is normally still ice free in December. In late December or early January of most years, a relatively warm period occurs, such

that the ice cover fails to increase in extent, even decreasing in some years (LaBelle et al. 1983). Then the ice extent and thickness both increase through late January and February, reaching maximums by mid-February to early March.

During colder winters the ice may extend into the Lower Inlet as far south as Anchor Point on the east side and Cape Douglas on the west side. The thickness of the ice pack varies between 0.5 and 2 m, apparently limited by the residence time of ice floes in the Inlet. Blenkarn (1970) reported that most of the ice in Cook Inlet is fine- to medium-grained with a bulk salinity of 4–6 ppt. He referred to previous studies, which indicated that most of the ice found in Cook Inlet is less than 30 days old, older ice having been transported out of the Inlet on the tides to the open ocean or having melted in transit. Based solely on Anchorage freezing degree-days (FDDs) over 30 winters, Blenkarn calculated that sea ice could grow to a maximum thickness of 0.66 m during the coldest 30-day period. Utt and Turner (1992) conducted a similar FDD analysis and found that the maximum ice thickness for the coldest 30-day period between 1931 and 1989 was 0.79 m.

Various rules of thumb for Cook Inlet ice conditions have been published. For example, substantial ice formation is said to begin after the Anchorage daily mean temperature drops below 20°F (–6.6°C) for the season (Blenkarn 1970) or when the seawater temperature cools to –1.1°C (Poole and Hufford 1982). According to the NWS, ice will completely clear from Cook Inlet approximately 21 days after the mean daily air temperature in Anchorage has risen above 0°C for the season (Schulz 1977b). However, the ice cover can vary significantly from year to year in terms of dates of onset and clearing, thickness, concentration, and extent of coverage.

Table 3 shows the variability in dates of onset and clearance for the 17-year period ending with the 1985–86 season. The date of the first significant ice occurrence and the springtime date of ice clearance are defined as the first and last occurrences for the season,



Figure 9. Typical mixed-ice conditions in Upper Cook Inlet, featuring ice floes, both level (un-deformed) ice and shove-thickened pans, interspersed with broken and brash ice in various first-year thin stages of development. (Photo by Orson Smith.)

respectively, of 10% ice concentration at the Phillips oil production platform, which is located approximately 14 km east of the North Foreland. Both dates varied by as much as two months over those years. The mean dates are November 25 and April 7, respectively, and the standard deviation for both is 17–18 days.

Poole and Hufford (1982) correlated several possible meteorological and oceanographic variables with the onset of ice in Cook Inlet for the 1970s decade. They analyzed factors such as FDDs, winds, precipitation amount, river discharge data, and coastal current inflow based on sea surface and air temperatures.

Degree-days

A “degree-day” is a means of describing the magnitude and duration of time that the mean daily air temperature differs from any specified temperature. In terms of sea ice formation, it is measured in either freezing degree-days (FDDs) that grow ice or thawing degree-days (TDDs) that melt ice. Every degree of temperature that the mean daily temperature departs from a given base value is one degree-day. For example, if we specify a base value of 0°C and the mean air temperature for a day is –10°C, then 10 Celsius FDDs have accumulated over the course of that day. Conversely a mean daily air temperature of +10°C would equal a 10-TDD accumulation. One Celsius degree-day equals 1.8 Fahrenheit degree-days. The number of FDDs and TDDs are summed separately and continuously over the entire winter season (from October 1 to April 30). The base value for the melting or growth of ice is arbitrary but is often chosen to best fit empirical data for the region of interest. The ice thickness models employed in Section 3.3 base the total thickness of ice grown or melted on the accumulated number of degree-days at monthly intervals during the winter.

Table 3. Dates of first significant ice and ice-out for northern Cook Inlet (defined as 10% ice concentration at the Phillips Platform). Extreme minimum and maximum dates are in bold. The 1984-85 season experienced an initial ice-out and refreeze on Feb. 13th. (After Brower et al. 1988.)

<i>Ice season</i>	<i>First Ice</i>	<i>Ice-Out</i>
1969-70	Nov 18	Mar 23
1970-71	Oct 17	May 7
1971-72	Nov 23	May 15
1972-73	Nov 13	Apr 10
1973-74	Nov 18	Apr 6
1974-75	Nov 24	Apr 9
1975-76	Nov 12	Apr 10
1976-77	Dec 17	Apr 9
1977-78	Nov 20	Mar 18
1978-79	Dec 16	Mar 31
1979-80	Dec 12	Mar 26
1980-81	Dec 6	Mar 10
1981-82	Nov 20	Apr 19
1982-83	Nov 29	Mar 21
1983-84	Dec 14	Mar 20
1984-85	Dec 17	Feb 13
	Feb 13	Apr 17
1985-86	Nov 5	Apr 18
Mean \pm s.d.*	Nov 25 \pm 17 days (Nov 8 – Dec 12)	Apr 7 \pm 18 days (Apr 9 – Apr 25)
Median*	Nov 23	Apr 9
Earliest*	Oct 17	Mar 10
Latest*	Dec 17	May 15

*Assumes only the first “First Ice” period and last “Ice-Out” period for the 1984-85 season.

Although the number of years studied was small (11 winters) and the scatter large, one relationship was found to be significant. Ice formation in the Upper Inlet correlated reasonably well with Anchorage FDDs, using a base of -3.9°C . Their analysis showed the Lower Inlet to be much less well correlated. These data are shown in Table 4 and plotted in Figure 10.

The hydrodynamic and meteorological environments are responsible for the large quantity of ice that is produced annually in Cook Inlet. The long season of freezing temperatures, the large tidal range, the high current velocity, and the shallow bottom depths all favor ice production. The latter three make for a turbulent water column and continuous surface flux that inhibits the growth of a stable ice cover, which can act as an insulating blanket and prevent heat exchange to

the atmosphere. While the latter three factors remain nearly constant from year to year, the fact that ice conditions are highly variable from season to season indicates that other factors are involved. The ice conditions are also related to topographic, meteorological, oceanographic, and sometimes even geological phenomena. The factors that can vary greatly and typically favor ice growth (Brower et al. 1988) include

- Radiational cooling,
- Cold, freshwater influx from stream flow discharge,
- Snow falling on the sea surface and melting, and
- Cold air mass advection.

On the other hand, many factors discourage ice growth in Cook Inlet. Examples of the more predictable are

Table 4. Dates of first significant ice for Upper (defined as 10% ice concentration at the Phillips Platform) and Lower Cook Inlet (undefined), and corresponding freezing degree-days (FDDs) at Anchorage and Kenai, respectively. Using the base value of -3.9°C to calculate FDDs yielded the best correlation for ice formation in the Upper Inlet. Extreme values are in bold. (After Poole and Hufford 1982.)

<i>Ice season</i>	<i>Upper Inlet first ice</i>	<i>FDDs (Base -3.9°C)</i>	<i>Lower Inlet first ice</i>	<i>FDDs (Base -3.9°C)</i>
1969-70	Nov 18	179	Dec 19	140
1970-71	Nov 21	161	Dec 15	167
1971-72	Nov 23	182	Dec 2	127
1972-73	Nov 13	176	Dec 14	185
1973-74	Nov 18	206	Dec 9	307
1974-75	Nov 24	166	Dec 29	216
1975-76	Nov 12	233	Dec 11	409
1976-77	Dec 10	131	—	—
1977-78	Nov 20	185	Dec 2	310
1978-79	Dec 16	120	Dec 22	188
1979-80	Dec 12	141	Dec 18	160
Mean \pm s.d.	Nov 25 \pm 12 days (Nov 13–Dec 7)	171 \pm 33	Dec 14 \pm 9 days (Dec 5–Dec 23)	221 \pm 91
Earliest	Nov 12		Dec 2	
Latest	Dec 10		Dec 29	

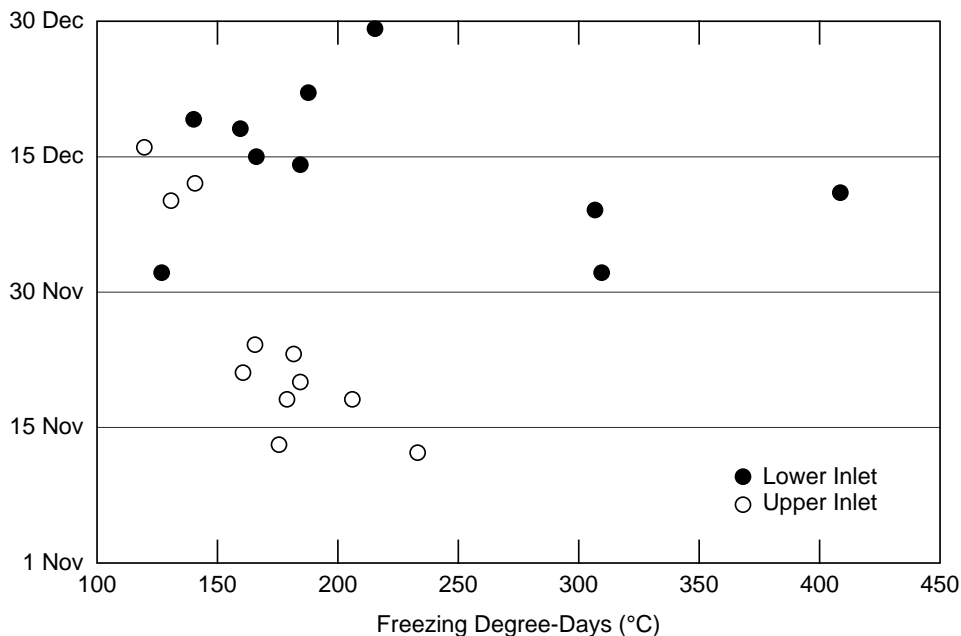


Figure 10. Dates of significant ice formation at the Phillips Platform with respect to freezing degree-days (assuming a base temperature of -3.9°C). Anchorage FDDs were used for the Upper Inlet, and Kenai data were used for the Lower Inlet. (After Poole and Hufford 1982.)

- The twice-per-day tides bringing in warm, saline water from the Gulf of Alaska,
- The tides moving ice from freshwater areas where it grows more rapidly to more saline water where it tends to melt, and
- North- and northeast-trending winds during the winter, which move ice down-Inlet to areas of melting.

Less-predictable negative factors include the incidence and amounts of solar radiation and snow cover on the ice. Also, southern air masses with above-freezing air temperatures can sometimes blanket the region for days at a time, causing rapid decay of a well-established ice cover. Occasionally volcanic eruption has been known to melt the ice cover. This was indeed the case in January 1976, when an eruption of Mount St. Augustine during a 5-day period raised the water temperature at the Dolly Varden platform (approximately 24 km NNE of West Foreland) from -2.2° to $+1.0^{\circ}\text{C}$. At the same time the ice concentration in the Inlet reportedly went from 95% to less than 50% (Schulz 1978).

Compared to other arctic regions where multi-year ice and icebergs occur, Cook Inlet ice conditions might be considered mild. However, they are significant because the first offshore developments in ice-infested waters for the petroleum industry were built in Cook Inlet. Four oil fields and one natural gas field were developed in the early 1960s in Upper Cook Inlet. The first fourteen offshore drilling and production platforms were built during 1964–1968 (Visser 1992), and environmental data necessary for their design were largely nonexistent. Some of the earliest ice environment studies in Cook Inlet were financed by the petroleum industry to ensure that the structures were constructed to withstand the forces imposed by the moving ice pack. The fact that there are now hundreds of platform-years of performance experience without a major failure testifies to the competence of the structural designs. Several published sources describe the data, procedures, and assumptions that engineers used to design the offshore and along-shore structures in Cook Inlet (e.g., Blenkarn 1970, Sanderson 1988, Visser 1992, Utt and Turner 1992, Bhat and Cox 1995). Visser (1992) listed parameters that governed design of the original platforms and compared them with recommended guidelines that were later adopted by the American Petroleum Institute (API 1988). These are shown in Table 5. The original design assumed a level, undeformed ice thickness of 1.1 m, which the API later amended to 0.6–0.9 m in its guidelines. The API also recommends a design thickness of 1.2–1.5 m for rafted ice.

Table 5. Ice design criteria for Cook Inlet petroleum industry platforms. (After Visser 1992, p. 148.)

<i>Design parameter</i>	<i>Design Criteria</i>	
	<i>Original design</i>	<i>API (1988) Recommended</i>
Ice thickness, level ice (m)	1.1	0.6–0.9
Ice thickness, rafted ice (m)	NA	1.2–1.5
Compressive strength, unconfined (MPa)	3.8	3.4–4.1
Compressive strength, confined (MPa)	300	275–330
Maximum load (MN)	42×10^6	40×10^6

3.3 Theoretical ice growth and melt

Sea ice growth and decay is a highly complex subject that relates to a wide array of environmental factors, such as air temperature, solar input, salinity of the water and the ice, and exposure to wind, waves, and tides. In Cook Inlet it is especially difficult to predict ice conditions because of the extreme magnitudes and constant fluctuation of the variables discussed in Section 3.2. However, since Poole and Hufford (1982) determined a reasonable correlation between accumulated FDDs and Upper Inlet freeze-up, temperature appears to be the best single indicator of the severity of the ice season. In this section we calculate theoretical ice sheet thickness values for Cook Inlet using simple models based on the average air temperatures in Anchorage. The models assume that when the mean daily air temperature is less than a specified value, ice will form, and when the temperature is higher than a specified value, the ice will melt.

LaBelle et al. (1983) stated that Brewster’s calculations of ice growth in Cook Inlet were made using a reformulation of Zubov’s (1945) model:

$$I^2 + 50I = 8R \quad (1)$$

where I is the ice thickness (cm) and R is the number of freezing degree-days that had accumulated in Anchorage, assuming a base temperature of 0°C . Solving the quadratic equation in the manner of Bowditch (1979) yields a form of the equation from which the ice growth, I_g , can more easily be determined as a function of the sum of FDDs. That is,

$$I_g = \frac{(2500 + 32R)^{0.5} - 50}{2}. \quad (2)$$

At the beginning of the ice season, the mean air temperature usually fluctuates above and below freezing for several days, if not weeks, before remaining below freezing. During this time the ice cover may oscillate between freezing and melting several times before becoming permanent. Bowditch stated that Equation 2 is to be applied after that initial fluctuation period. According to LaBelle et al. (1983), the first significant ice does not form in Cook Inlet until after an initial accumulation of 33.3 FDDs, probably to account for this fluctuation period. This stipulation causes Equation 2 to become

$$I_g = \frac{[2500 + 32(R - 33.3)]^{0.5} - 50}{2} \quad (3)$$

which we used to calculate the ice thickness values in Table 6.

Also in the manner of LaBelle et al., we calculated theoretical ice melt for Cook Inlet, I_m , using the relationship of Bilello (1980):

$$I_m = 0.93 (TDD) \quad (4)$$

where I_m is in centimeters and TDD is the accumulated thawing degree-days using a temperature base of -1.8°C . However, Bilello empirically derived Equation 4 using data from 12 Canadian sites and only 1 Alaskan site to give the thickness decrease of a fast ice sheet from its maximum thickness.

The calculated monthly values for I_m in Table 6 show that above-freezing mean air temperatures can occur at any time during the winter season and that TDDs will cause departure from the theoretical ice growth relationship (eq 3). Of course, the reverse is also true—FDDs occurring at any time during the thaw period will result in a departure from the melt calculated by Bilello's equation. The reader is therefore cautioned to consider the I_g and I_m values in the table only as indicative of the relative severity of ice conditions in Cook Inlet throughout the ice season. This is especially true for FDDs during October and April and for TDDs during the rest of the season, as shown by their higher standard deviations.

In Table 6 we summed FDDs with respect to 0°C and TDDs with respect to -1.8°C to be consistent with the stated method of LaBelle et al. (1983). Figure 11 shows the mean monthly FDD and TDD totals for 1973–1997 for four locations on Cook Inlet (Fig. 1). In general, Kenai is the coldest site—it accumulates the most FDDs and the fewest TDDs over the winter

period. Anchorage closely follows Kenai, with approximately 14% fewer FDDs and 7% more TDDs during the winter season. The other two sites illustrate the moderating effect that proximity to the Gulf of Alaska has on air temperature. Homer, near the southern end of Cook Inlet, has significantly milder air temperatures in winter than Kenai and Anchorage, with about half the FDDs and about 60% more TDDs. Kodiak, located south of Cook Inlet in the Gulf of Alaska, has about one-fifth the FDDs and about two and a half times the TDDs of Anchorage and Kenai.

The season totals of FDDs and TDDs for the period of record (POR) are shown in Figure 12. Year-to-year variability is substantial at all four stations. There was no statistically significant long-term trend of warming or cooling at any of the sites based on these data.

The FDD record for Anchorage compiled by LaBelle et al. (1983), together with the more recent data of this report, is shown in Figure 13. The data sets match closely during the period that they overlap (1974–1982). Least-squares linear fits through the respective data sets show opposite trends. The earlier data exhibit a marked warming trend of -11 FDD/yr, whereas the later time frame shows a slight cooling trend of $+4$ FDD/yr.

3.4 Cook Inlet marine ice data

Ice conditions in Cook Inlet have been routinely reported since the 1969-70 winter season as an aid to navigation. Annual reports were published throughout the 1970s by the Alaska Region Headquarters of the NWS in Anchorage (Hutcheon 1972a, b, 1973; Schulz 1977a, b, c, 1978; Eaton 1980; Poole 1980, 1981a, b). These were post-season reports that typically provided a qualitative description of the ice conditions as they related to specific weather phenomena, air temperature, and FDDs recorded at Anchorage. They also provided the historical dates of the first significant ice formation and the end-of-the-season ice-out dating back to the 1969-70 season. Although similar ice reports were apparently not published after the 1979-80 season, the dates of ice formation and ice-out continued to be compiled by the NWS up through the 1985-86 season (Table 3).

In December 1984 the NWS in Anchorage began sporadic analysis and forecasting of the extent, concentration, and stage of development of Cook Inlet ice. With the importance of commercial navigation, fishing, and tourism access to remote sites around Cook Inlet, the practice continues today with even greater scientific discipline and regularity. The NWS has provided regular ice reports since 1989 for Alaskan coastal and offshore waters. Since 1994 Russell Page has held the position of ice forecaster for that region and has developed numerous tools to aid in the

Table 6. Accumulated freezing and thawing degree-days at Anchorage, Alaska, and calculated sea ice growth and melt in Cook Inlet. The degree-day data were provided by AFCCC and are for January 1973 to December 1997, inclusive. (These differ from the values shown in LaBelle et al. because of their incorrect derivation and/or application of Equation 3.)

Season	Oct		Nov		Dec		Jan		Feb		Mar		Apr	
	FDD	TDD	FDD	TDD	FDD	TDD	FDD	TDD	FDD	TDD	FDD	TDD	FDD	TDD
1972-73							473	1	279	5	131	35	0	124
1973-74	31	84	291	0	224	11	404	0	255	2	170	53	1	153
1974-75	7	104	157	28	205	3	337	18	301	8	165	11	23	84
1975-76	41	142	268	1	329	7	255	18	292	17	129	19	12	113
1976-77	44	121	46	61	142	6	27	76	23	73	113	17	17	128
1977-78	11	181	243	0	343	2	174	14	103	38	57	51	2	172
1978-79	3	191	86	32	168	19	142	5	301	0	31	71	0	168
1979-80	0	217	34	103	343	3	312	18	84	38	93	42	0	178
1980-81	7	153	67	26	531	3	41	60	127	39	11	94	3	129
1981-82	6	128	176	16	263	8	419	0	254	11	116	37	33	93
1982-83	107	47	178	9	193	27	265	2	159	12	67	42	6	147
1983-84	17	110	112	14	248	2	232	23	191	4	10	129	0	167
1984-85	22	128	193	5	220	11	49	44	281	11	93	21	103	70
1985-86	90	102	289	4	102	52	114	12	164	23	139	24	76	88
1986-87	13	179	126	41	88	47	160	22	94	17	123	50	1	151
1987-88	15	187	78	17	231	7	231	4	141	23	29	44	8	136
1988-89	30	87	179	2	180	18	474	3	224	3	151	21	1	171
1989-90	41	117	242	17	137	23	284	17	428	3	88	37	1	189
1990-91	34	83	346	0	288	1	287	23	196	18	141	19	3	144
1991-92	38	91	119	27	192	1	186	12	256	3	146	47	33	123
1992-93	42	72	103	46	290	14	282	4	174	18	62	28	0	198
1993-94	9	172	132	51	131	17	174	17	233	16	141	52	17	170
1994-95	46	111	257	6	264	5	270	4	174	19	244	23	0	192
1995-96	2	162	173	15	219	7	438	1	247	1	68	38	13	167
1996-97	140	56	205	4	314	1	278	16	33	39	125	2	3	159
1997-98	37	62	78	43	238	6								
Mean	33	123	167	23	235	12	252	17	201	18	106	40	14	145
St. Dev.	33	46	83	24	93	13	125	18	92	17	54	27	24	34

Season	Oct		Nov		Dec		Jan		Feb		Mar		Apr	
	I_g	I_m	I_g	I_m	I_g	I_m	I_g	I_m	I_g	I_m	I_g	I_m	I_g	I_m
1972-73							39.4	1.0	5.9	4.7	2.2	32.6	0.0	115.7
1973-74	0.0	78.0	26.8	0.0	21.4	10.3	34.9	0.0	5.4	2.1	3.3	49.1	0.0	142.1
1974-75	0.0	97.1	15.1	26.4	19.7	3.1	30.3	17.1	6.4	7.8	3.2	10.3	0.0	78.5
1975-76	1.1	131.8	25.0	0.5	29.7	6.2	24.0	17.1	6.2	15.5	2.2	17.6	0.0	105.4
1976-77	1.7	112.6	1.9	56.8	13.7	5.2	0.0	70.3	0.0	68.2	1.7	16.0	0.0	118.8
1977-78	0.0	168.4	23.0	0.0	30.7	1.6	16.9	12.9	1.4	35.7	0.0	47.5	0.0	160.2
1978-79	0.0	177.7	7.3	29.5	16.2	17.6	13.6	4.7	6.4	0.0	0.0	66.1	0.0	156.6
1979-80	0.0	201.5	0.1	95.6	30.7	3.1	28.4	17.1	0.8	35.1	1.1	39.3	0.0	165.3
1980-81	0.0	142.6	4.9	23.8	42.9	3.1	1.1	55.8	2.1	36.2	0.0	87.8	0.0	120.4
1981-82	0.0	119.4	17.0	15.0	24.6	7.2	35.9	0.0	5.4	9.8	1.8	34.1	0.0	86.8
1982-83	9.9	43.9	17.2	8.8	18.6	24.8	24.8	1.6	3.0	11.4	0.2	38.8	0.0	136.4
1983-84	0.0	102.3	10.4	12.9	23.4	2.1	22.0	21.7	3.8	3.6	0.0	119.9	0.0	155.5
1984-85	0.0	118.8	18.6	4.7	21.0	10.3	2.4	40.8	6.0	9.8	1.1	19.1	1.4	65.1
1985-86	7.8	94.6	26.7	3.6	9.2	48.6	10.6	10.9	3.1	21.2	2.5	22.2	0.5	81.6
1986-87	0.0	166.4	12.0	38.2	7.6	43.4	15.5	20.7	1.1	16.0	2.0	46.5	0.0	140.5
1987-88	0.0	174.1	6.4	15.5	22.0	6.7	21.9	4.1	2.5	21.2	0.0	40.8	0.0	126.6
1988-89	0.0	80.6	17.3	2.1	17.4	17.1	39.5	2.6	4.7	3.1	2.8	19.6	0.0	158.6
1989-90	1.2	109.0	22.9	16.0	13.1	21.2	26.3	16.0	8.9	2.6	0.9	34.6	0.0	175.7
1990-91	0.2	77.0	30.9	0.0	26.6	1.0	26.5	21.2	4.0	16.5	2.5	18.1	0.0	133.8
1991-92	0.8	84.7	11.2	25.3	18.5	1.0	17.9	11.4	5.4	3.1	2.6	43.9	0.0	114.7
1992-93	1.4	67.2	9.4	42.4	26.8	12.9	26.1	4.1	3.4	17.1	0.1	26.4	0.0	184.5
1993-94	0.0	159.7	12.6	47.0	12.5	16.0	16.9	16.0	4.9	14.5	2.5	48.6	0.0	158.1
1994-95	2.0	103.3	24.1	5.2	24.7	4.7	25.2	3.6	3.4	18.1	5.1	21.2	0.0	178.3
1995-96	0.0	150.4	16.8	14.0	21.0	6.2	37.2	0.5	5.2	0.5	0.3	35.7	0.0	155.0
1996-97	13.4	51.7	19.7	4.1	28.6	0.5	25.8	14.5	0.0	36.2	2.1	2.1	0.0	148.3
1997-98	0.6	57.4	6.3	39.8	22.6	5.2								
Mean	1.6	114.8	15.3	21.1	21.7	11.2	22.5	15.4	4.0	16.4	1.6	37.5	0.1	134.5
St. Dev.	3.4	42.6	8.2	22.2	7.6	12.2	11.0	17.0	2.2	15.5	1.3	24.7	0.3	32.0

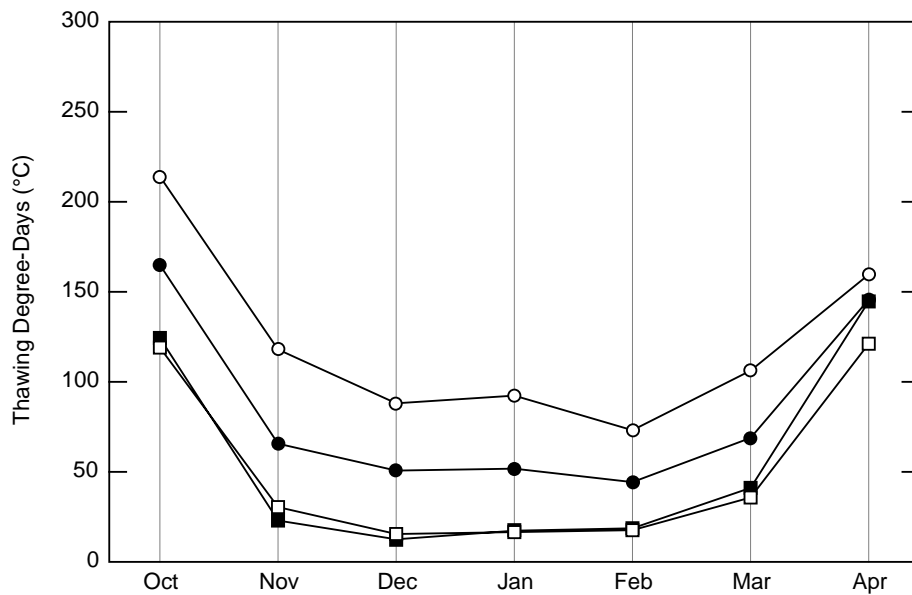
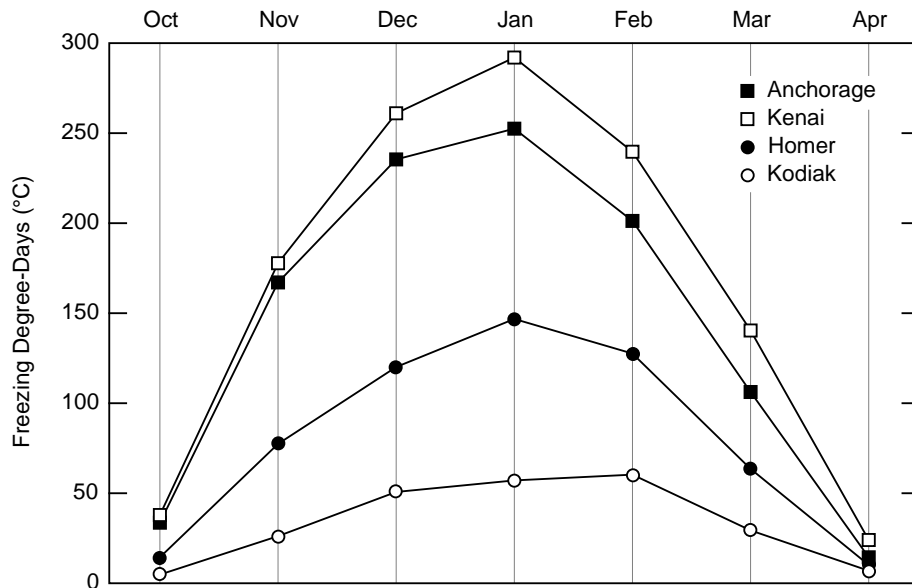


Figure 11. Mean monthly freezing and thawing degree-days for 1974–1997 assuming base temperatures of 0 and -1.8°C , respectively, for four locations on Cook Inlet.

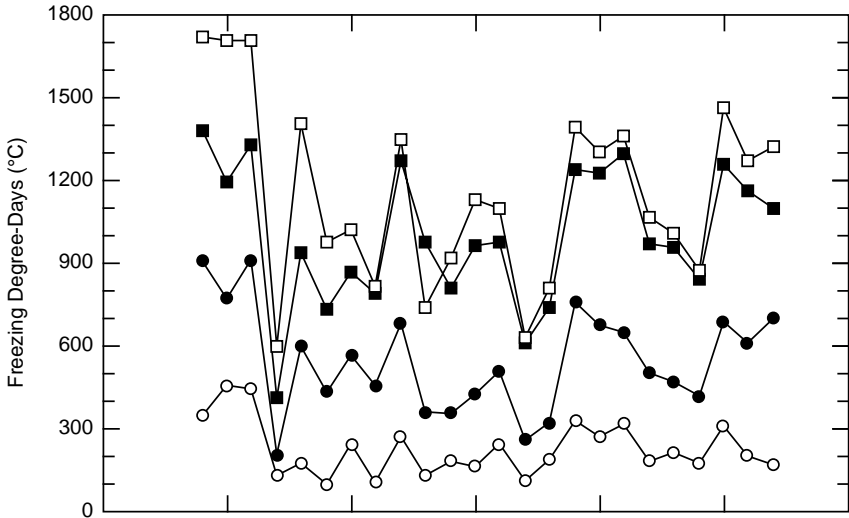


Figure 12. Seasonal variation of freezing and thawing degree-days for 1974–1997 for four locations on Cook Inlet.

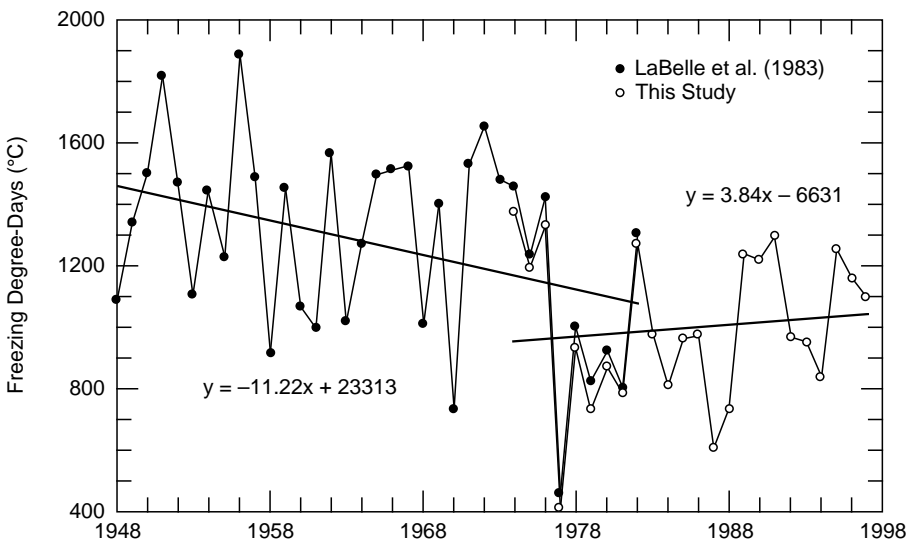
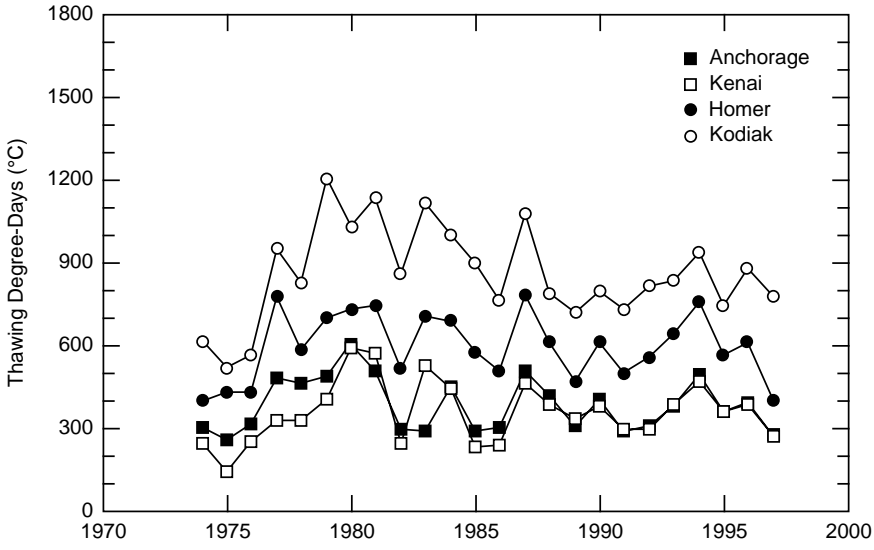


Figure 13. Season total FDDs for Anchorage, Alaska. The 1948–1982 data, reported by LaBelle et al. (1983), are compared with those for 1974–1997 obtained for this study from Air Force Combat Climatology Center (AFCCC). Opposite trends in mean temperature are evident.

creation of more accurate, detailed, and consistent reports (Page 1997). He has developed a network of reliable observers upon whom he regularly calls to verify remote sensing information. In addition to five-day forecasts, the NWS in Anchorage issues year-round graphic analyses of current sea ice conditions and sea surface temperatures. Scheduled sea ice analyses and five-day sea ice forecasts are produced Monday, Wednesday, and Friday, and a sea surface temperature chart of Alaskan waters is produced each Tuesday and Thursday. Annotated satellite analyses of sea surface temperatures and sea ice are produced when clear skies allow these features to be observed. These latest products are available for viewing at their Internet website.* Visual and infrared images from Advanced Very High Resolution Radiometer (AVHRR) sensors aboard several satellites are received directly by the Anchorage NWS. Images from satellite-borne Special Sensor Microwave/Imager (SSM/I) and synthetic aperture radar (SAR) are also available through the National Ice Center or the University of Alaska Fairbanks after signal processing routines for ice perception are executed by these agencies.

Winter's extended darkness and low sun angles during daylight hours make visual images difficult to interpret. The most reliable imagery for interpreting ice conditions during the winter when sun angles are low is infrared. SSM/I and SAR images are not available directly and require special processing and interpretation, which makes them inconvenient for regular operational use. Ground-level inspection of Turnagain Arm conditions, for example, has on several occasions revealed open water when these images implied an ice cover. The majority of NWS winter analyses are based on AVHRR infrared images of about 1-km resolution. Conditions perceived from this imagery are verified whenever possible with ground-level inspection and observer reports at the Port of Anchorage, Nikiski, and occasionally oil platforms and vessels in Cook Inlet.

The National Ice Center (NIC) in Washington, D.C., also produces routine ice analyses for Cook Inlet on a semi-weekly schedule (Tuesdays and Fridays) throughout the ice season. Appendix B shows an example of an ice analysis that was produced by the NIC, along with their explanatory material for interpreting the image. These analyses generally differ only slightly from those produced by the NWS†. Indeed the NIC and NWS ice analysts maintain at least weekly contact to share data sources and interpretation. The NIC

analyst relies primarily on SAR imagery with a resolution of 10–300 m to begin developing his forecasts and analyses (Fig. 14). If the SAR imagery doesn't exist or is ambiguous, he can also draw upon AVHRR imagery or the Defense Meteorological Satellite Program Operational Linescan System's (DMSP OLS) visible and infrared imagery (with a resolution of 0.5–3 km). NIC ice reports are generally more conservative than the NWS reports, reporting somewhat higher concentrations and older, thicker ice. The NIC's entire archive (123 digital images by the end of the 1999–2000 season) is available for viewing and downloading at their website,* whereas only the single latest NWS chart is similarly available.

Because of its longevity the NWS ice analysis archive was selected over the NIC database for the mapping of the sea ice in Cook Inlet. Despite some irregular gaps in the record, 673 NWS charts through the 1998–99 season were available for analysis, an example of which is shown in Figure 15. For example, no charts were on file for the 1985–86 season until January, there were only two charts for the entire 1986–87 season, and there were none for all of 1996. Minor gaps are apparent during other years as well, and it is not known whether reports have been lost or if none were issued during those periods. The record is particularly irregular for November and April, but this was not unexpected for the months of freeze-up and melt-out. Because of this uncertainty in the data record at the beginning and end of the ice season, only the NWS ice charts that were issued between the beginning of December and the end of March were used. Accordingly no attempt was made to estimate the time of onset or termination of the ice cover.

Currently the NWS Cook Inlet ice chart archive is maintained on microfiche at the Alaska State Climate Center in Anchorage. For this atlas, each archived chart was digitally scanned to create an image that could then be analyzed quantitatively using GIS software. Within the GIS architecture, each image was rectified and registered to a standard base map that portioned Cook Inlet into equal-area grid cells. Numerical values representing the particular ice concentration and stage of development were assigned to each cell. The data from the images were accumulated into biweekly intervals, and statistical operations were conducted to show the mean ice conditions in terms of concentration and stage of development, and the zones of ice occurrence probability for Cook Inlet. These calculated data were used to produce the ice maps shown on the following pages. The calculation procedure is more fully described in Appendix C.

*<http://www.Alaska.net/~nwsfoanc/>

†Craig Evanego, National Ice Center, Washington, D.C., personal communication, October 24, 2000.

*<http://www.natice.noaa.gov/>



Figure 14. Radarsat-1 SAR imagery showing the Forelands area of Cook Inlet at near low tide on December 30, 1998. The region appearing stippled along the East Foreland is 6 to 10 tenths young and first-year thin sea ice. Tidal flats are visible along the northern shores with streaks of 5 to 7 tenths new ice forming just offshore in Trading Bay and Redoubt Bay. The bright white specks in three distinct rows that appear in the water north of the Forelands are oil production platforms. [Image copyright by Canadian Space Agency (1998); used by permission.]

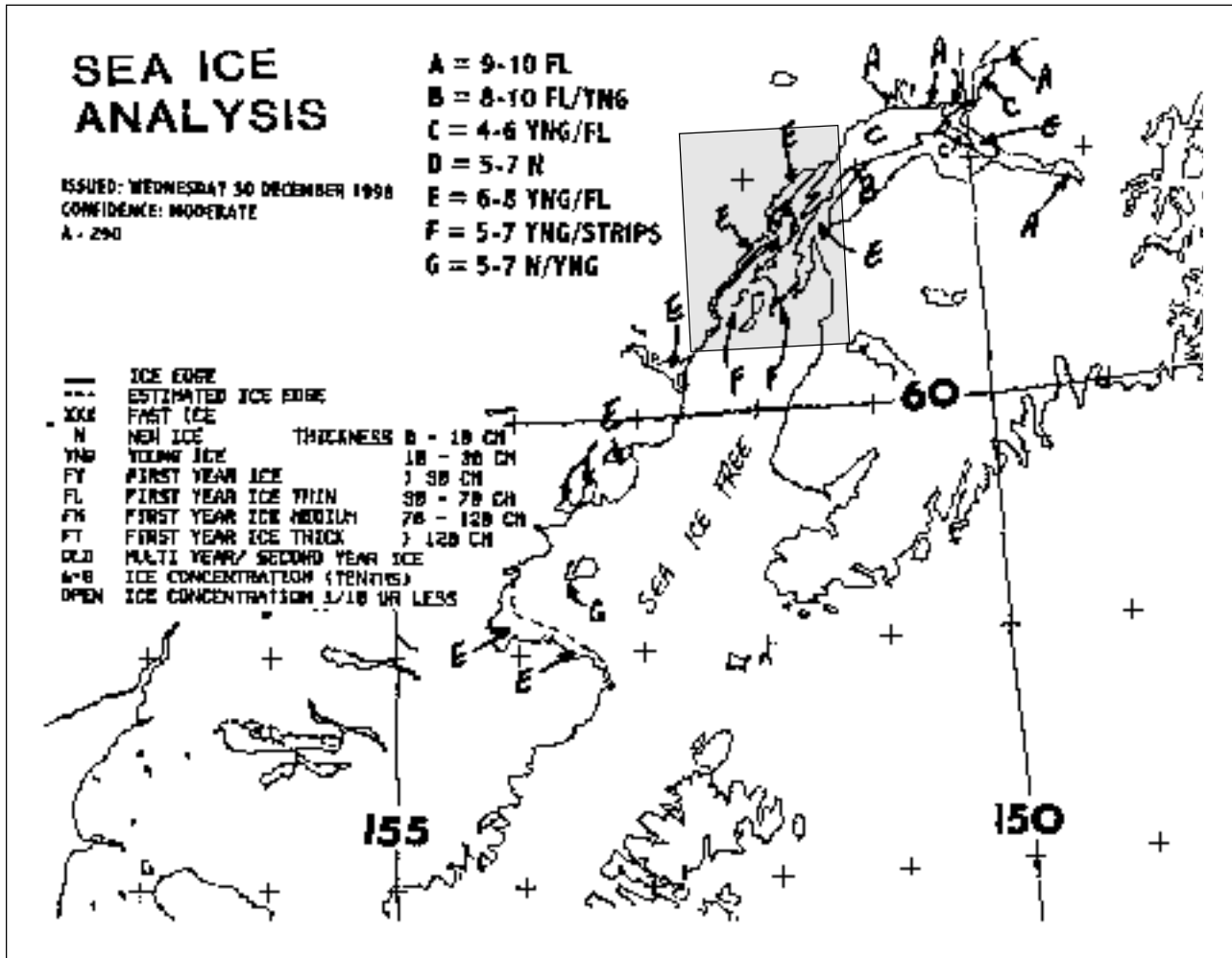


Figure 15. Example of a sea ice analysis chart issued by the Alaska Region Headquarters of the National Weather Service. Regions of similar ice type are assigned the same code letter by the NWS forecaster, and a key is placed in an open area on the chart. The code letters may change from chart to chart, as their purpose is simply to provide an abbreviated way to define the regions and avoid clutter on the report. This particular analysis was produced using, among other tools, the SAR image shown in Figure 14. The shaded rectangle shows the image footprint over the Inlet.

4 EXPECTED ICE CONDITIONS

The following Map Set 1 shows the mean ice conditions for the period of record (January 1986 to April 1999) for each biweekly interval between 1 December and 31 March. These were calculated simply from the arithmetic mean of ice concentration and stage of development. Map Set 2 shows the probability of occurrence of any ice, regardless of concentration or stage of development, and shows the 0%, >25–50%, >50–75%, and >75–100% zones of ice occurrence probability. Map Set 3 shows the same zones of probability of ice occurrence but for ice of at least 5/10ths concentration. The process by which these maps were derived is explained in Appendix C.

The use of the different map sets depends on the particular application of interest. The most comprehensive information is contained in Map Set 1, which shows two different ice variables: mean ice concentration (indicated by color) and mean stage of development (indicated by hatching pattern). Concentration is a relative measure of the water surface that is actually covered with ice. Stage of development provides a general indication of the ice thickness and its integrity, or strength. Both conditions are important and necessary for mariners who need to know whether a particular region might be navigable at a particular time during an average ice year.

Map Sets 2 and 3 show only the probabilities of ice occurrence, without respect to its stage of development. By extension, they indicate the extreme minimum and maximum regions of ice extent for two ice concentration levels. For example, an interest in knowing where in Cook Inlet any ice has occurred, regardless of concentration, would require the use of Map Set 2. The extreme limit of occurrence of any ice is denoted by the boundary between the 0% occurrence and the >0–25% occurrence. In other words, during the most severe ice year, the maximum extent of ice

would be encountered near this boundary. Similarly, the regions with the highest likelihood of any ice are indicated by the >75–100% occurrence zones. These zones are highly probable of having ice, even during the least severe ice years.

Map Set 3 shows the same probability zones of occurrence but for a more severe ice condition, that of at least 5/10ths concentration. Certain applications of interest may depend not simply on the mere presence of any ice, but may require the additional knowledge of its concentration. For example, certain vessel navigations may be affected only when ice concentrations are 5/10ths or greater, and certain behaviors of marine animals, fish stocks, and waterfowl may be similarly dependent. As with Map Set 2, during a very severe ice year, 5/10ths ice concentration may be encountered at the boundary between 0% and >0–25% occurrence. Likewise, during minimum ice years, 5/10ths or greater ice concentrations are very likely to occur within the >75–100% occurrence zones.

It is important to remember that these maps were developed from ice charts that the NWS constructed using a combination of remote sensing observations and visual reports. While the NWS uses a wide range of available tools to construct their charts as accurately as possible, that accuracy is limited by the amount and resolution of the available data. For example, small amounts of ice could exist outside the 0% probability boundary, because these amounts may have been too small to be observed visually or detected by remote sensing during the initial NWS analysis. The following maps are therefore not meant for actual navigation or for any other purpose upon which their accuracy may be relied for the safety of life or property. They are simply statistical representations of the ice conditions as reported by the NWS for the period of record.

Pages 26 to 52 contain Map sets 1–3

[TO MAP SETS](#)

5 OCEANOGRAPHY

5.1 Bathymetry

The bottom topography of Cook Inlet is, in general, extremely rugged, with dramatic changes in elevation. It has many relatively deep locations adjacent to shoals (Fig. 16). However, the depth of the Inlet is generally less than 73 m (40 fathoms). Near the mouth of the Inlet, the bottom drops away steeply to a general depth of 183–366 m (100–200 fathoms) near the Barren Islands.

Significant portions of Knik and Turnagain Arms are exposed at low tide. Several extensive tidal flats are located in the Head and Upper Inlet (Fig. 17). The largest of these are the Susitna Flats, near the mouth of the Susitna River; Potter Flats, south of the city of Anchorage; Chickaloon Flats, east of Point Possession; and Palmer Hay Flats, at the northern end of Knik Arm.

Of the many rivers that discharge into the Inlet, three contribute about 70% of its total freshwater input. These are the Knik, Matanuska, and Susitna Rivers, and all find their way into the Upper Inlet via the Susitna Lowland. These rivers are the outwash drainages for large glaciers, and consequently each transports a heavy burden of sediment, especially during the summer months, when discharge volume is high. The surface waters draining into Knik Arm deposit a total of 20 million tons of sediment per year, while the annual sediment discharge into Turnagain Arm is only about 3 million tons (Gatto 1976). Because of the volume of sediment delivered, the southern third of Knik Arm, which serves as the shipping approach to the Port of Anchorage, is only about 18–36 m (10–20 fathoms) deep mid-channel. At the entrance to Knik Arm lies a stable shoal with a mean lower low water (MLLW) depth of 8.5 m (28 ft) over which deep-draft traffic to and from Anchorage must pass during high

tide. The U.S. Army Corps of Engineers excavates about 172,000 m³ of silt from the Port's maneuvering area each year to maintain –35 ft MLLW level (USACE 1993).

Between the Forelands the water reaches a depth of 124 m (68 fathoms). The channels to the east and west of Kalgin Island attain depths of 73 and 121 m (40 and 66 fathoms), respectively. Similar depths are not found elsewhere north of the 50-fathom isoline (NOS 1997). South of the 50-fathom contour, the bottom drops away steadily such that the three entrances to Cook Inlet have depths exceeding 183 m (100 fathoms).

5.2 Currents and tides

Throughout the year the strong Alaska Current trends northwesterly along the Canadian and Alaskan coastlines, bringing southern waters to the Cook Inlet region. This marine water enters the Inlet via the Stevenson and Kennedy Entrances and mixes to varying degrees, depending on the season and meteorological conditions, with the fresh water draining from the land and mountains surrounding the Inlet. The incoming ocean water is relatively clear and saline compared to the outflowing surface drainage. During the summer months, melting snow and surface runoff cause a net freshwater outflow of more than 100,000 m³/s from the Inlet to the Gulf of Alaska. During the winter months, low air temperatures and the production of ice shrink the volume and velocity of river runoff substantially. The mean and extreme flow volumes for the three largest rivers emptying into the Upper Inlet are shown in Table 7. River sediment delivery diminishes during the low-flow period, and the Inlet's outflow becomes equal to its inflow (Murphy et al. 1972). This hydrologic exchange, superimposed on re-

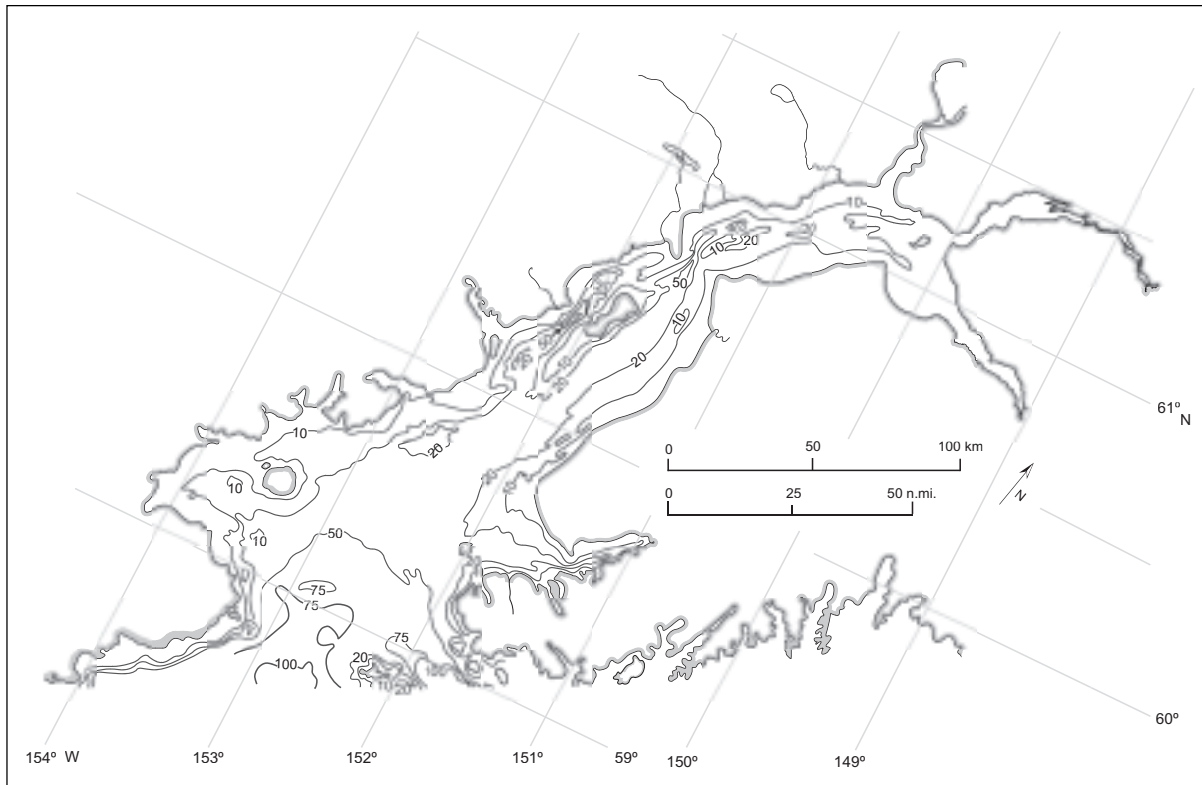


Figure 16. Cook Inlet bathymetry.

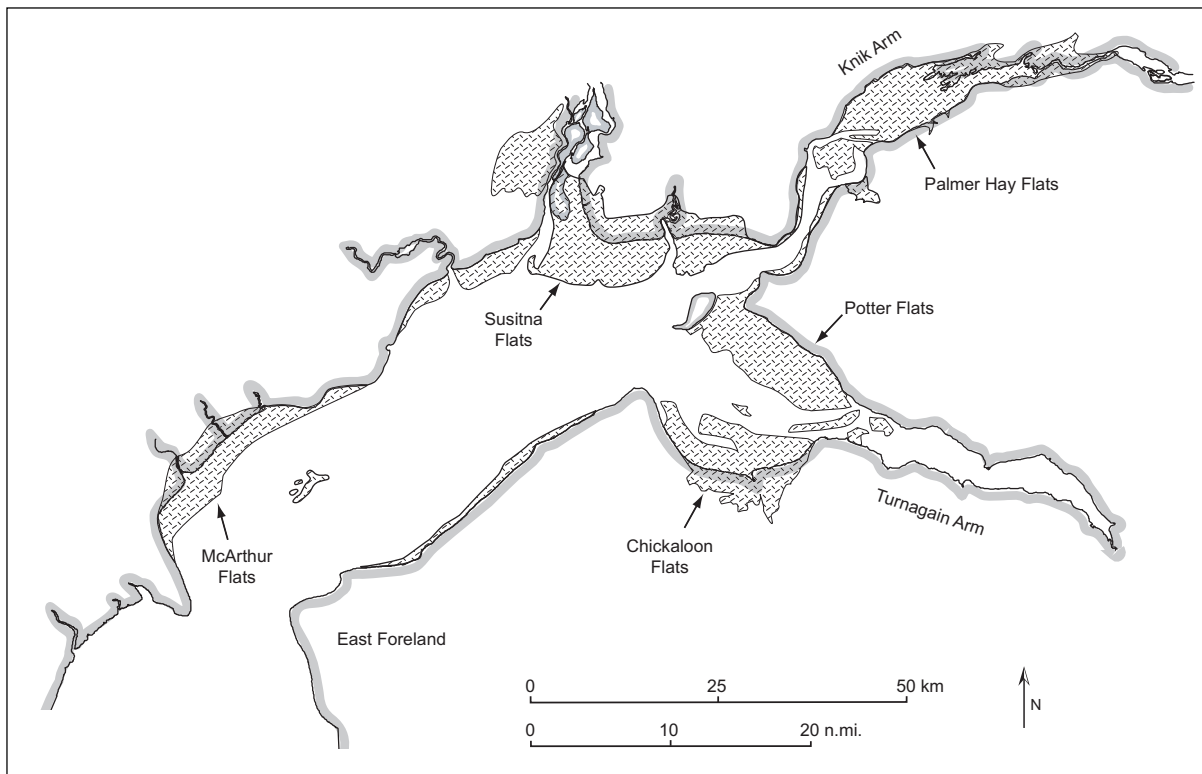


Figure 17. Tidal mudflats in Upper Cook Inlet and the Head Region. (After Raney 1993.)

Table 7. Stream flow data for the Matanuska, Knik, and Susitna Rivers. (After USACE 1993, p. 22.)

<i>River</i>	<i>Gauge location</i>	<i>Minimum flow (m³/s)</i>	<i>Average flow (m³/s)</i>	<i>Maximum flow (m³/s)</i>
Matanuska	Palmer	6.68	108.3	2,324.8
Knik	7 mi S. of Palmer	7.36	19.5	10,166.8
Susitna	1.5 mi downstream of Yentna River confluence	141.6	1,436.8	8,834.9

circulating tidal currents, follows the counterclockwise net circulation pattern shown in Figure 18. The warmer and clearer oceanic water moves up the Kenai Peninsula side of the Inlet, while the cold and sediment-laden fresh water flows toward the Gulf along the western side. Mean background currents (i.e., those superimposed on tidal flow) are dominated by meteorological events with time scales on the order of 3–4 days (Muench et al. 1978) and are strongest on the western side of the Inlet. Although the background currents near the surface have greater velocities than those deeper, they are still an order of magnitude

weaker than the tidal currents. The southward net flow attains its peak intensity of about 0.2 m/s (0.4 knots) in summer and its minimum of about 0.1 m/s (0.2 knots) in winter. At the same time the net flow of saline Gulf water on the eastern side moves northward at 0.02–0.05 m/s (0.04–0.1 knots) to replace the western outflow (Weingartner 1992). Between these opposing flows is a shear zone in which a portion of the northward inflow is continually being drawn into the southward outflow. This summer flow pattern for Lower Cook Inlet is illustrated in Figure 19.

The Lower Inlet tends to be stratified in both tem-

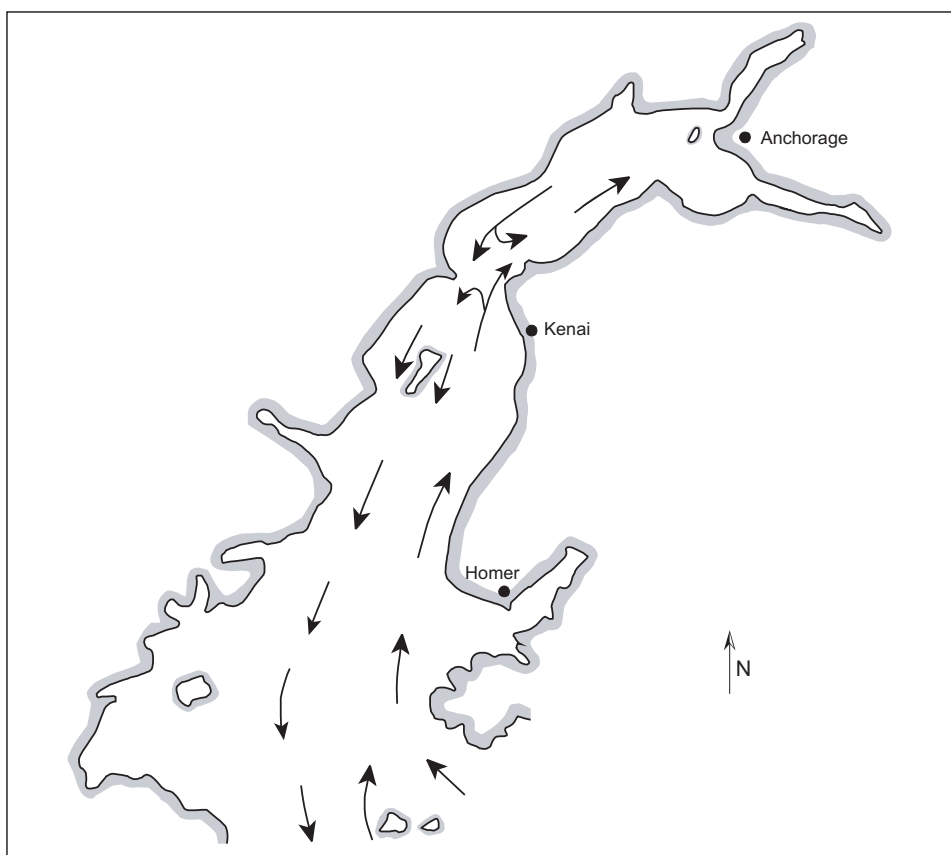


Figure 18. General surface circulation pattern in Cook Inlet. (After USACE 1993.)

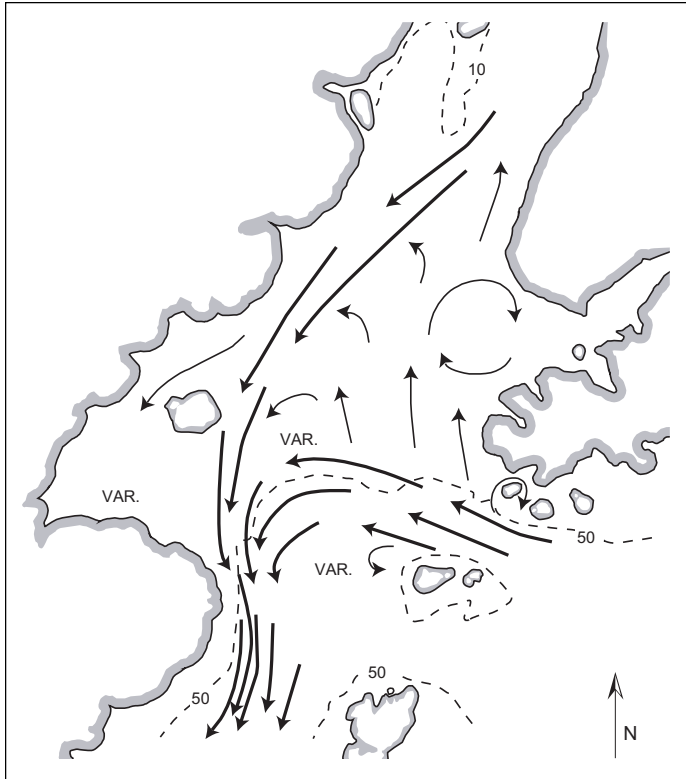


Figure 19. Summer surface circulation pattern in Lower Cook Inlet as proposed by Muench et al. (1978). Variable currents are evident near the mouth and in Kamishak Bay. The 10- and 50-fathom isobaths are indicated by the dashed lines.

perature and salinity. During summer, water on the western side is more distinctly stratified than on the eastern side, with warmer, fresher Inlet waters overlying the colder, saltier oceanic water. North of the Forelands the water column is uniformly mixed due to turbulence caused by the large tidal range and high current velocities over relatively shallow basin depths. While the entire water column mixes vertically with each tidal cycle in the Upper Inlet, this is not the case horizontally. In the Upper Inlet, incoming water still tends to move northward along the eastern side, while fresher, more turbid water flows southward out along the western side.

Southward net flow follows the western shore in the Upper Inlet, around both the east and west sides of Kalgin Island and along the western half of the Lower Inlet. The net southward flow splits at Augustine Island, with a branch diverting through Kamishak Bay before rejoining the main flow off Cape Douglas. The net southward flow then exits the Inlet via Shelikof Strait (Rappeport 1982). Maintained in suspension by tidal currents, fine clay- and silt-sized sediment particles are primarily transported out of the Inlet through Shelikof Strait to the Aleutian Trench beyond Kodiak Island.

The tides dominate gross circulation and turbulent intensity in the Inlet. According to Gatto (1976) the tidal regimes of the Upper and Lower Inlet are different and both quite complex. Tidal predictions at An-

chorage are derived from computations using 114 frequency constituents, more than any other tidal station in the U.S. (Smith 2000).

The tidal currents in Upper Cook Inlet are rectilinear or reversing. That is, the changing tides are marked by a period of slack water, or no current, before accelerating in the opposite direction. In the Lower Inlet the tidal currents are classified as rotary in that they never completely go slack between ebb and flood tides. Instead they diminish at low and high water and change direction while rotating around to the opposite direction (Gatto 1976). In general, maximum tidal currents are 1.0–1.5 m/s (2–3 knots) in the Lower Inlet, increasing to over 2 m/s in the Upper Inlet. According to AEIDC (1974), tidal currents range from 0.5 to 3.1 m/s (1 to 6 knots) and average 2.0 m/s (3.8 knots) between the East and West Forelands, the narrowest point of the Inlet. Spring tides* can result in 4.1-m/s (8-knot) tidal currents near constrictions, such as between the Forelands, between Harriet Point and the south

*So named, not because of the time of year in which they occur, but because the tides seem to leap or “spring” higher during those times of the month when the sun and moon are aligned. Conversely, when the moon is perpendicular to the alignment of the earth and sun, “neap tides,” that is, the smallest tides of the month, occur.

Site	Map Location	Tidal Range			
		Mean		Diurnal	
		(m)	(ft)	(m)	(ft)
Ushagat Island	1	3.47	11.4	4.18	13.7
Nordyke Island	2	3.93	12.9	4.63	15.2
Port Chatham	3	3.63	11.9	4.36	14.3
Oil Bay	4	3.84	12.6	4.24	13.9
Homer	5	4.79	15.7	5.52	18.1
Snug Harbor	6	4.02	13.2	4.79	15.7
Ninilchik	7	5.09	16.7	5.82	19.1
Drift River Terminal	8	4.69	15.4	5.52	18.1
Kenai River	9	5.39	17.7	6.31	20.7
North Foreland	10	5.58	18.3	6.40	21.0
Anchorage	11	7.89	25.9	8.78	28.8
Sunrise	12	9.24	30.3	10.15	33.3

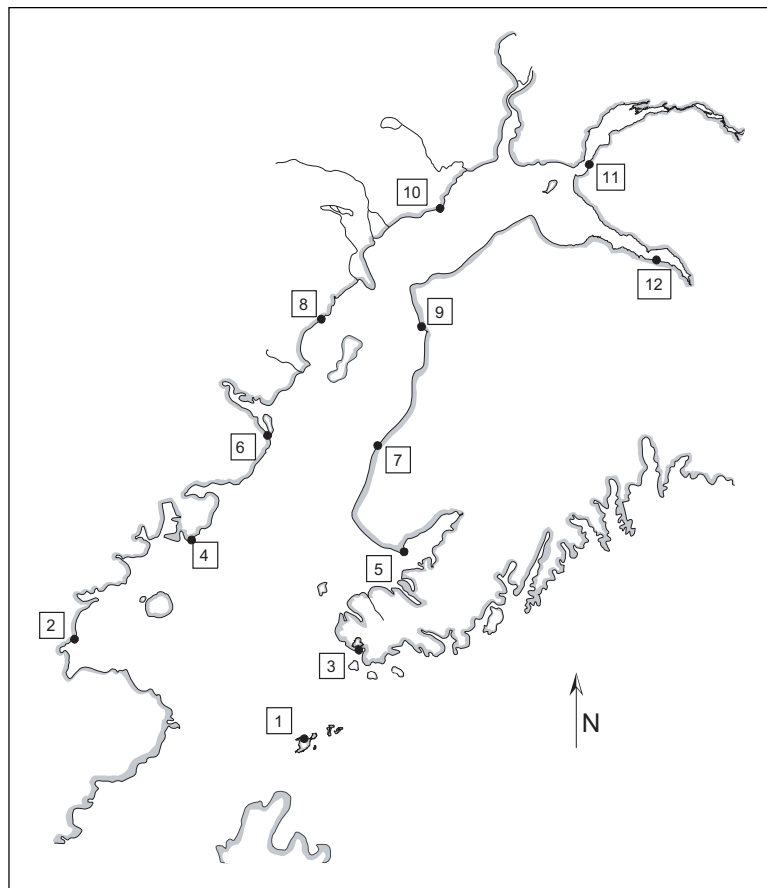


Figure 20. Tidal ranges at various locations around Cook Inlet. The mean tidal range is the difference in height between the mean high water and the mean low water levels. The diurnal tidal range is the difference between the mean higher high water and the mean lower low water levels.

end of Kalgin Island, and at the mouths of Knik and Turnagain Arms (NOS 1994, Nelson 1995). All of Turnagain Arm experiences very strong currents, and the tide often comes in as a tidal bore with a wave height of up to 1.8 m (6 ft) (NOS 1994).

The extreme tidal changes that occur in Cook Inlet are exceeded in magnitude only by those occurring in the Bay of Fundy in eastern Canada. The phenomenon is mainly due to resonance. That is, the Inlet water's natural period of oscillation closely matches that of the astronomical tides (Raney 1993, Pearce et al. 1999). The tides are semi-diurnal in that there are two high and two low tides of unequal height (a "diurnal inequality") in each lunar day of 24 hours and 50 minutes. From the entrance to the head of the Inlet, there is a 4.5-hour lag

in water level response to the tides. The tidal range varies greatly depending on location, as shown in Figure 20. From north to south the mean water level fluctuation varies from 3.47 m (11.4 ft) at Kennedy Entrance to 7.89 m (25.9 ft) at Anchorage. The greatest tidal ranges occur during spring tides, when the mean ranges are exceeded by more than 1.5 m (5 ft). Extreme tidal ranges at the upper ends of Knik and Turnagain Arms are as high as 12 m (39.4 ft) (Rappeport 1982, Nelson 1995). Large east-to-west tidal differences are caused by the Coriolis effect, which produces higher tide levels along the eastern shoreline. For example, the mean tidal range is 3.84 m (12.6 ft) at Oil Bay and 4.79 m (15.7 ft) at Homer, which are equal in latitude but on opposite sides of the Inlet.

6 CLIMATOLOGY

Alaska experiences four distinct climatic zones (AEIDC 1974)—Arctic, Continental, Transition, and Maritime (Fig. 21). While the weather conditions in each zone can vary dramatically from normal, the zones can be characterized by general patterns. Meteorological conditions in the Arctic zone (extending from the Brooks Range northward to the Arctic Ocean) are primarily influenced by the inflow of cold, polar air masses. Winds along the northern coast are strong but diminish with distance inland.

Most of interior Alaska is Continental in climate. This region is distant from ocean waters, so the climate is drier and air temperatures fluctuate considerably more, both seasonally and diurnally. Summer temperatures are generally quite high, while winter temperatures can be extremely low. Precipitation and winds are relatively light.

The weather in the Maritime zone is dominated by the presence of nearby ocean waters. Air temperatures are moderated year-round by the proximity of oceanic water. Because of the enormous heat capacity of the nearby ocean waters, summer air temperatures are lower and winter temperatures are significantly higher than in areas that are more inland. In addition, the ocean acts as a large source of moisture, resulting in much more precipitation along the coast as rain in summer and snow in winter, especially in windward, higher-elevation areas. A maritime climate is also characterized as having persistently strong surface winds.

The Transition zone is generally the narrow region between the Continental and Maritime zones, where the climatic conditions are something between the two sets of conditions that exist in the adjacent zones. Cook Inlet predominantly experiences a Maritime climate; however, the blocking effect of the Kenai Peninsula

and its mountains produces a more Transition-type climate, especially in the upper reaches of the Inlet. In addition, weather patterns and climate within the Cook Basin are affected by the warm Alaska Current; the shallow bathymetry of the Inlet; its high tidal variation and fast currents; and the Inlet's high north-to-south salinity gradient. These conditions prevent an intact ice cover from forming over the Inlet during winter. The broken ice cover and newly forming ice release heat from the water to the atmosphere, thus moderating the climate.

6.1 Source and description of climatological data for Cook Inlet

The meteorological information presented in this report was extracted, summarized, and supplied to us by the Air Force Combat Climatology Center (AFCCC) in Asheville, North Carolina. The stations selected for this study are the “first-order” NWS stations in the vicinity of Cook Inlet. First-order sites routinely record station parameters on an hourly basis throughout the year. Three of these stations—Anchorage, Kenai, and Homer—lie along Cook Inlet's eastern coastline, and the fourth—Kodiak—is located on an island in the Gulf of Alaska. Unfortunately, there are no first-order stations along the Inlet's western coast from which to obtain comparable long-term meteorological records. The stations are listed and described in Table 8.

Summary data for the four stations were compiled by AFCCC for January 1973 to December 1997. Monthly means, extremes, and occurrence frequencies for air temperature, wind speed, wind direction, and sea level pressure are shown in Appendices D, E, and G.

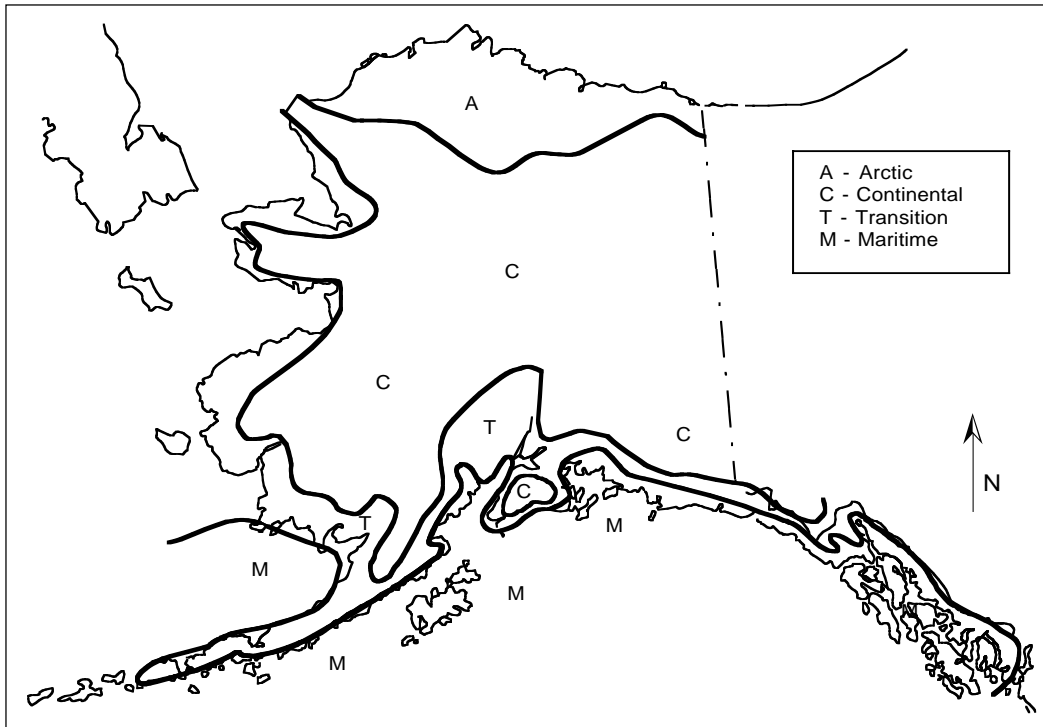


Figure 21. Alaska's climatic zones. (After AEIDC 1974.)

Table 8. Location and description of first-order Cook Inlet meteorological stations used in this study.

<i>Station name</i>	<i>Latitude (N)</i>	<i>Longitude (W)</i>	<i>Elevation (masl*)</i>	<i>Period of record</i>	<i>No. of observations</i>
Anchorage International Airport	61° 10'	150° 01'	39.9	Jan. 1, 1973– Dec. 31,1997	213,864
Kenai Municipal Airport	60° 34'	151° 15'	29.0	Jan. 1, 1973– Dec. 31,1997	207,577
Homer Municipal Airport	59° 38'	151° 30'	22.0	Jan. 1, 1973– Sep. 30, 1997	190,791
Kodiak	57° 45'	152° 30'	34.1	Jan. 1, 1973– Dec. 31,1997	207,669

*Meters above sea level.

6.2 Station climatologies

6.2.1 Anchorage International Airport

Anchorage International Airport, the most northern weather station polled for this study, is located near the northern end of Cook Inlet, where it branches into Knik and Turnagain Arms. Nearly 3.2 km equidistant from the Inlet on three sides (north, west, and south), Anchorage is situated in open, gradually up-sloping terrain characterized by marshes, shallow depressions, low knolls, and glacial moraine. Anchorage is considered to have a Transition-type climate but is the most Continental of the four stations used in this study. Approximately 16 km to the east, the broad valley enclosing Cook Inlet Basin rises abruptly to the 1,500–3,000-m- (5,000–10,000-ft-) high summits of the northeast-to-southwest-trending Chugach Mountains. The range inhibits the inflow of moist, maritime air from the Gulf of Alaska, so that precipitation in the Anchorage area is only 10–15% that of the region on the Gulf of Alaska side of the mountains (NCDC 2000a). For example, the mean annual precipitation for Anchorage is 40 cm, whereas it is 445 cm just 52 km to the southeast, at Whittier on Prince William Sound. Approximately 160 km from Anchorage, the Alaska Range encloses the Inlet's west, northwest, and north sides. During winter, these mountains help to shelter the basin from the inflow of cold, polar air from the north. Although the climate of the Anchorage area is moderated by the mountain ranges, the seasonal changes nevertheless are well defined. Prevailing winds during the summer are from the south, with the months of April and September marking the periods of wind shift between north and south.

The summer season is generally considered to last from late May through August. The warmest month is normally July, with a daily high temperature mean of 19°C and a daily low of 12°C (Fig. 22). The highest temperature recorded in each of June, July, and August from 1973 through 1997 was 27°C. Winds are normally light and southerly during the summer in Anchorage. The mean monthly wind speed for each month ranges between 3.0 and 3.9 m/s (5.9 and 7.6 knots), with May and June having the highest mean wind speeds (Fig. 22). Similarly, mean monthly maximum winds ranged from 5.3 to 8.5 m/s (12.3 to 16.6 knots), with May and June again having the strongest winds and the lowest frequency occurrence for calm wind observations (Fig. 22). Interestingly May is also the month with the least extreme wind speed on record (19.0 m/s; 37 knots). Since 1973 the highest recorded wind speed has been 31.9 m/s (62 knots) (March and July). After May the occurrence of rain increases (Fig. 22). During June through August, only about 5 days per month are predominantly clear, and the mean num-

ber of days per month with “measurable” precipitation (0.025 cm or more) is approximately 13. A predominantly clear day, in this application, is one in which the majority of that day's cloud-cover observations are categorized as only 0-2 oktas (zero to 2/8ths) overcast. Fifty-six percent of Anchorage's total annual precipitation occurs during July, August, September, and October (ACRC 1997a). The precipitation range shown in the figure represents the “near-normal” precipitation, that is, the middle 33% of the data for the 1961–1990 period of record. The data points within the range are the median precipitation values. Anchorage's growing season averages 124 days in length, with the first frost of fall occurring on September 16 on average. The earliest frost was recorded on August 16 (NOS 1994).

Autumn is considered to last from early September to mid-October, when below-freezing air temperatures and snowfall become more frequent. The mean monthly air temperatures for September and October are 10° and 2°C, respectively. From 1973 through 1997 these two months experienced mean totals of 2 and 18 days, respectively, when the daily low temperature was below freezing (Fig. 22). On average the mean daily air temperature remains below freezing after October 23 (NOS 1994). Northerly and southerly winds prevail, with nearly equal occurrence in September, and total more than 40% of all observations (see wind roses in Appendix E). Some southerly wind events (post-frontal winds that follow storms tracking northeastward out of the Bering Sea or Bristol Bay) can achieve damaging proportions in the Anchorage area. Less-frequent “Chugach” winds, which arrive from the southeast, accelerate through the Chugach Mountain passes, and funnel down canyon creeks, sometimes create gusts in excess of 47 m/s (92 knots). These can cause considerable structural damage. September has the highest total precipitation and the most days with measurable precipitation. Rainfall then drops off dramatically in October. Measurable snowfall is rare in September, but occasional snowfalls of 25 cm or more begin occurring in mid-October. The average date of first snowfall is October 15, but measurable snowfall has arrived as early as September 20 (NOS 1994).

Winter in Anchorage is generally considered to last from mid-October to early April, when lakes and streams are frozen over. It is a time of clear, cold weather alternating with mild, cloudy periods. Air temperatures decrease steadily into January, when daytime highs average around –5°C. The mean nighttime lows are near –11°C, but clear and cold winter nights can approach –30°C. The lowest temperature recorded from 1973 to 1997 was –34°C. Total annual freezing degree-days average 1008°C-days (1814°F-days).

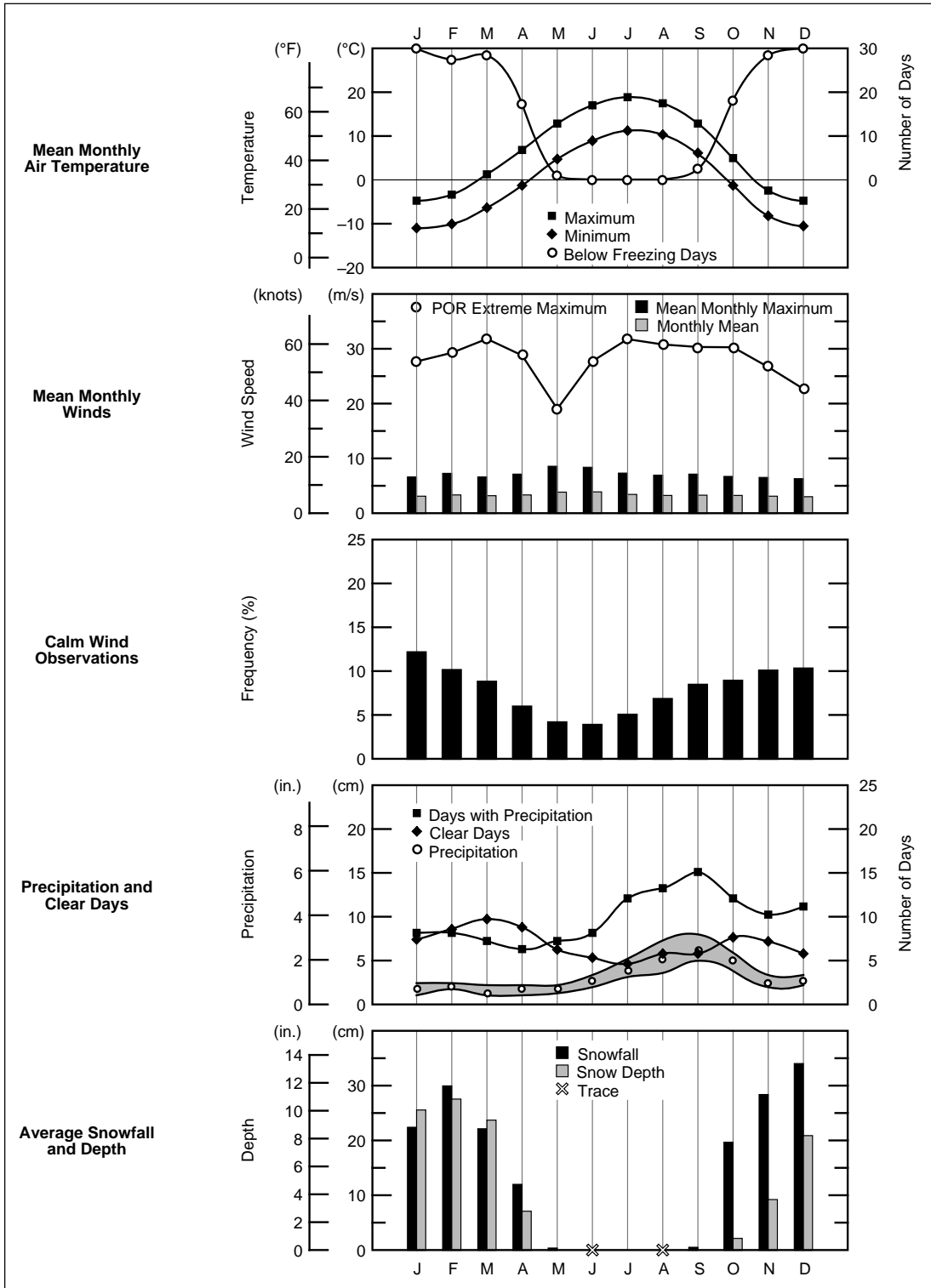


Figure 22. Weather summary for Anchorage International Airport. The POR is January 1973 to December 1997 except as follows: precipitation (1961–1990) (NCEP 2000), days with measurable precipitation (0.025 cm or more) (1967–1996), clear days (1973–1999), and snowfall and snow depth (1953–1999). The precipitation range is the middle 33% of the data for the 30-year POR; the data points are median values.

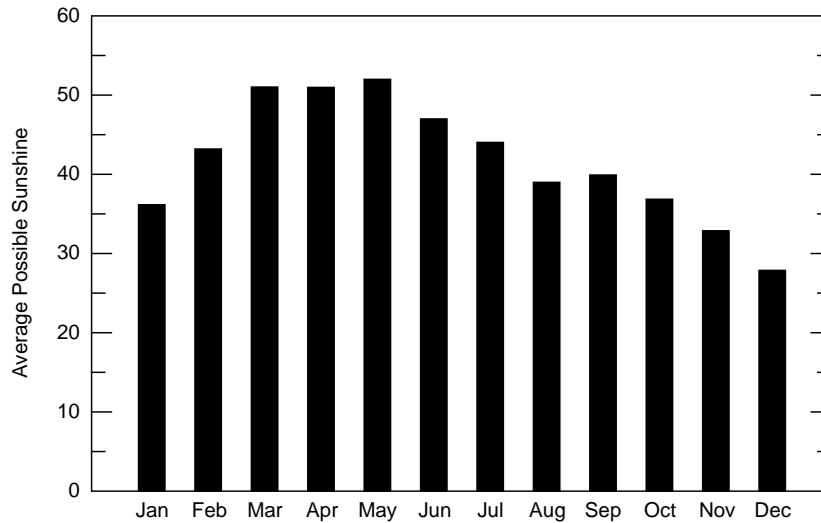


Figure 23. Average percent possible sunshine at Anchorage International Airport from 1955 to 1993. (After ACRC 1997a.)

North winds account for more than 30% of all observations during October through March. The second most prevalent winds during this period are from the northeast, accounting for an additional 15% of observations (see wind roses in Appendix E). Winds are normally light, but strong “Northers” occasionally result from rapidly deepening storms in the Gulf, when the Alaskan interior is dominated by a large, cold air mass. Rainfall sometimes occurs, but most precipitation in winter is in a frozen form. The average total snowfall in the Anchorage area lowlands ranges from 1.8 to 2.3 m annually (NCDC 2000a), with much greater amounts falling in the higher elevations of the Chugach Range. Winter typically arrives a month earlier and ends a month later from 300 to 600 m above sea level (asl). The snow in the Anchorage area is usually light and dry, having a low liquid water equivalent. It occurs on 20–25% of all midwinter days but usually comes in small daily amounts. Snowfall amounting to 10 cm or more occurs on only 2% of those days. Freezing rain and ice fogs are rare in Anchorage, but warmer fogs occur on an average of 15

days each winter (NCDC 2000a). The depth of snow on the ground rarely exceeds 38 cm; during January and February it averages about 27 cm (Fig. 22).

The mean daily temperature averages above freezing from April 8 to October 23 (NOS 1994). Spring-time conditions begin around the end of April with a predominance of warm days and cool nights and the disappearance of the snow cover. On average the last day in which the temperature drops below freezing is May 15, but it has been as late as June 6 (NOS 1994). March has the greatest number of predominantly clear days for all four Cook Inlet stations. April has the least number of days with measurable precipitation and the lowest monthly precipitation for the year (Fig. 22). Only about 13% of the annual precipitation total falls during March through May, and each of those months averages more than 50% total possible sunshine (Fig. 23). The average last date of measurable snowfall is April 14, but snow has fallen as late as May 6. As in September, north and south winds are equally prevalent in April and total more than 40% of all observations.

6.2.2 Kenai Municipal Airport

The town of Kenai is located at the mouth of the Kenai River, about 30 km south of the East Foreland and about 95 km south of Anchorage. It is a fishing town and a base of support for offshore drilling activities in Cook Inlet. Being closer to the Gulf of Alaska by both air and water, one would expect its climate to be more Maritime-like than that of Anchorage. This is the case with its winds, which are slightly stronger and more consistent from month to month. However, its precipitation and temperature patterns are similar to those of Anchorage.

The daily high temperatures follow those of Anchorage very closely throughout the year, and the daily lows are only slightly lower than in Anchorage. In summer, mean air temperatures in Kenai range from about 6°C overnight to 17°C during the day (Fig. 24). The extreme maximum temperature is 30°C and was recorded in August. Mean monthly winds at Kenai show relatively constant mean and maximum speeds throughout the year (Fig. 24). The mean monthly maximum winds are about 15 knots year round, but for a slight dip in July and August. The frequency of calm wind observations falls to its lowest levels during May through July (Fig. 24). On average, calm winds are twice as likely year round to occur at Kenai as at Anchorage.

Rainfall within the Inlet region begins to increase after June with the shift in wind direction to the southwest quadrant, bringing moisture in from the Gulf of Alaska. The mean annual precipitation total at Kenai is 43 cm, with September again having the highest monthly mean (Fig. 24). The number of days per month with measurable precipitation peaks in September. However, the number of predominantly clear days per month remains relatively constant all year round, rang-

ing only between 7 and 11 days.

Autumn is the rainy season, when the prevailing surface winds shift around to the northeast for the remainder of the year. From the July low of 15%, the frequency of north and northeast winds increases steadily to the high of 65% in February. September, October, and November frequencies are 39, 54, and 62%, respectively. The frequency of calm wind observations reaches its annual peak in November, when nearly one-quarter of all wind readings are calm. Although snow falls in lesser amounts in Kenai than in Anchorage, apparently less of it melts, so mean snow depths are greater than those in Anchorage (Fig. 24).

Minimum air temperatures during the coldest part of the winter in Kenai average -13°C , about 2.5°C lower than Anchorage. An extreme minimum temperature of -43°C occurred in January during the period 1973–1997. During that POR, Kenai experienced a mean annual freezing degree-day total of 1168°C-days ($2102^{\circ}\text{F-days}$). The mean monthly frequency of calm wind observations, in general, declines steadily throughout the winter and into spring. Monthly precipitation levels drop off in the late fall and remain low throughout the winter and spring, as do the number of days per month with measurable precipitation. Kenai's mean snow depth exceeds its snowfall from January through March.

Springtime arrives along with warmer days and rapidly increasing daylight duration. The driest months of the year are typically March and April, which total only 3.6 cm of the station's 43-cm annual precipitation total. The mean daily air temperature typically rises above freezing in April, and the mean number of days per month in which freezing temperatures are observed decreases sharply from 25 in April, to 9 in May, to only 1 in June.

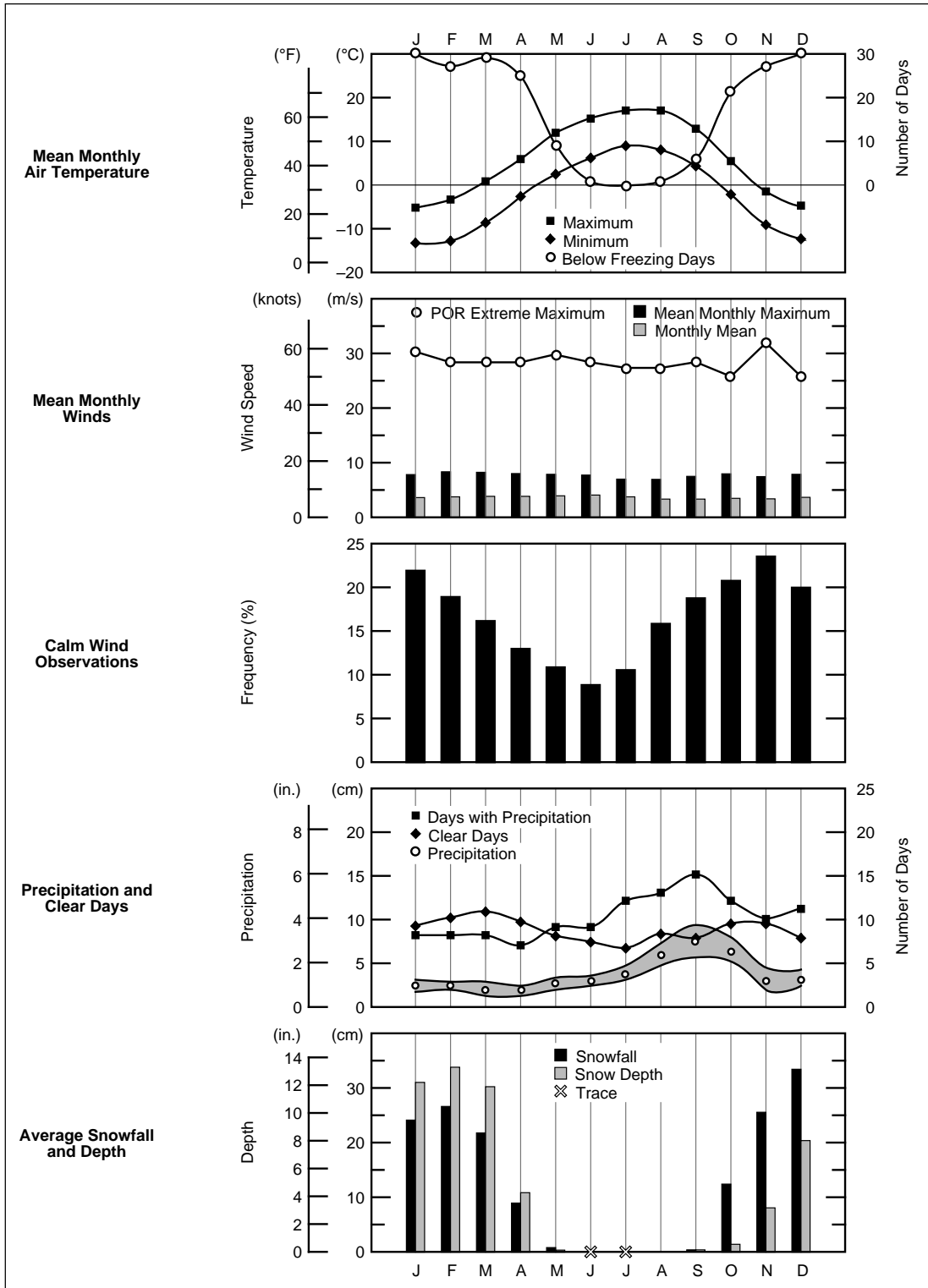


Figure 24. Weather summary for Kenai Municipal Airport. The POR is January 1973 to December 1997 except as follows: precipitation (1961–1990) (NCEP 2000), days with measurable precipitation (0.025 cm or more) (1967–1996), clear days (1973–1999), and snowfall and snow depth (1953–1999). The precipitation range is the middle 33% of the data for the 30-year POR; the data points are median values.

6.2.3 Homer Municipal Airport

The community of Homer is located in the Lower Cook Inlet region, 105 km southwest of Kenai and about 195 km from Anchorage. Homer Airport is situated at the head of Coal Bay on the northern shore of the much-larger Kachemak Bay (NCDC 2000b). The coastal shoreline on either side of the station curves northward so that water lies within 2 km to the east, south, and west. The terrain for a distance of about 2.4 km immediately to the northwest through northeast rises gradually to 150 m (500 ft) above sea level before rising abruptly to 305 m (1000 ft) at about a distance of 3.2 km. The nearest 460-m (1500-ft) elevation is Lookout Mountain, which lies 6.4 km to the north-northeast. The nearest 610-m (2000-ft) elevation lies within the foothills of the Kenai Mountains, 19.3 km to the southeast and across Kachemak Bay. The southwest-to-northeast-trending Kenai Mountains, with 1220- to 1830-m (4000- to 6000-ft) summit elevations, are 24–37 km distant.

Homer enjoys a transitional climate intermediate to that of Kenai and Kodiak in terms of temperature and precipitation. Mean and extreme monthly wind speeds are very similar to those at Kenai. Monthly precipitation amounts are greater than at Kenai but are still significantly less than at Kodiak because of the shelter afforded by the Kenai Range. Homer's total annual precipitation amounts to about 65 cm, which is about half the amount that falls on the Alaskan Gulf side of the mountains. Being situated closer to the moderating waters of the Gulf of Alaska, Homer's diurnal and seasonal air temperatures are less dramatic and variable than in Anchorage. Summers are cooler and winters are warmer than in Anchorage.

During the warmest months of July and August, daytime highs average slightly below 16°C and lows are about 10°C (Fig. 25). Although the extreme maximum temperature (31°C) for 1973–1997 was recorded in May, July's extreme high is 27°C. Mean monthly winds are similar in magnitude to those at Kenai. The monthly maximum wind speeds, excluding gusts, are relatively consistent from month to month at around 15 knots (Fig. 25). The wind speeds are lowest and the frequency of calm winds is high during July and August (Fig. 25). The prevailing wind directions during June through August are west and southwest (see wind roses in Appendix E). However, from July until September, there is an increasing frequency of northeast winds. The frequency and amount of precipitation begins trending upward at the end of June, typical of

the entire Cook Inlet region (Fig. 25). The total annual precipitation (about 65 cm), however, is 60% higher than in Anchorage, yet the mean number of days per year with measurable precipitation (144) is only 23% higher.

On average the first frost occurs in Homer by mid-September. September and October have 4 and 18 days, respectively, during which the mean air temperature never rises above freezing. The monthly mean air temperatures for those months are 9° and 4°C, respectively (ACRC 1997b). Nearly 50% of the winds in September are from the north, northeast, or east. The frequency increases to 60% for October, and the trend becomes even stronger in winter, when approximately 70% of all November, December, and January winds are out of the northeast quadrant. The greatest precipitation amounts occur in autumn. More than 25% of the annual total falls during September and October, and half of the days during these two months experience measurable precipitation. Homer's first snowfall typically occurs in late September, but snowfalls often change to rain throughout the winter.

Homer's winter monthly air temperatures average near –4°C, some 4°C degrees warmer than in Anchorage. Monthly mean highs for the months of December, January, and February are only slightly below freezing, and the mean lows are –6°C. January is the coldest month in Homer, with a monthly mean of –3.6°C. The extreme lowest temperature recorded in Homer between 1973 and 1997 was –31°C. As was mentioned, northeast winds dominate throughout the winter, and the wind directions become more variable in the spring. Mean monthly precipitation amounts decrease steadily throughout the winter and spring. The average annual snowfall is about 140 cm, with the greatest monthly amounts occurring in December and February (Fig. 25). The average depth of snow on the ground is highest in February.

March and April are characterized by a rapid decrease in the frequency of days with below-freezing air temperatures and a rapid increase in hours of daylight. The frequency percentage of wind out of the southwest quadrant increases steadily during February, March, April, May, and June (15, 25, 36, 47, and 55%, respectively). There is also a decrease in the frequency of calm wind observations accompanying this shift in wind direction. Monthly precipitation decreases during the spring, as does the frequency of cloudy and partly cloudy days, and days with measurable precipitation.

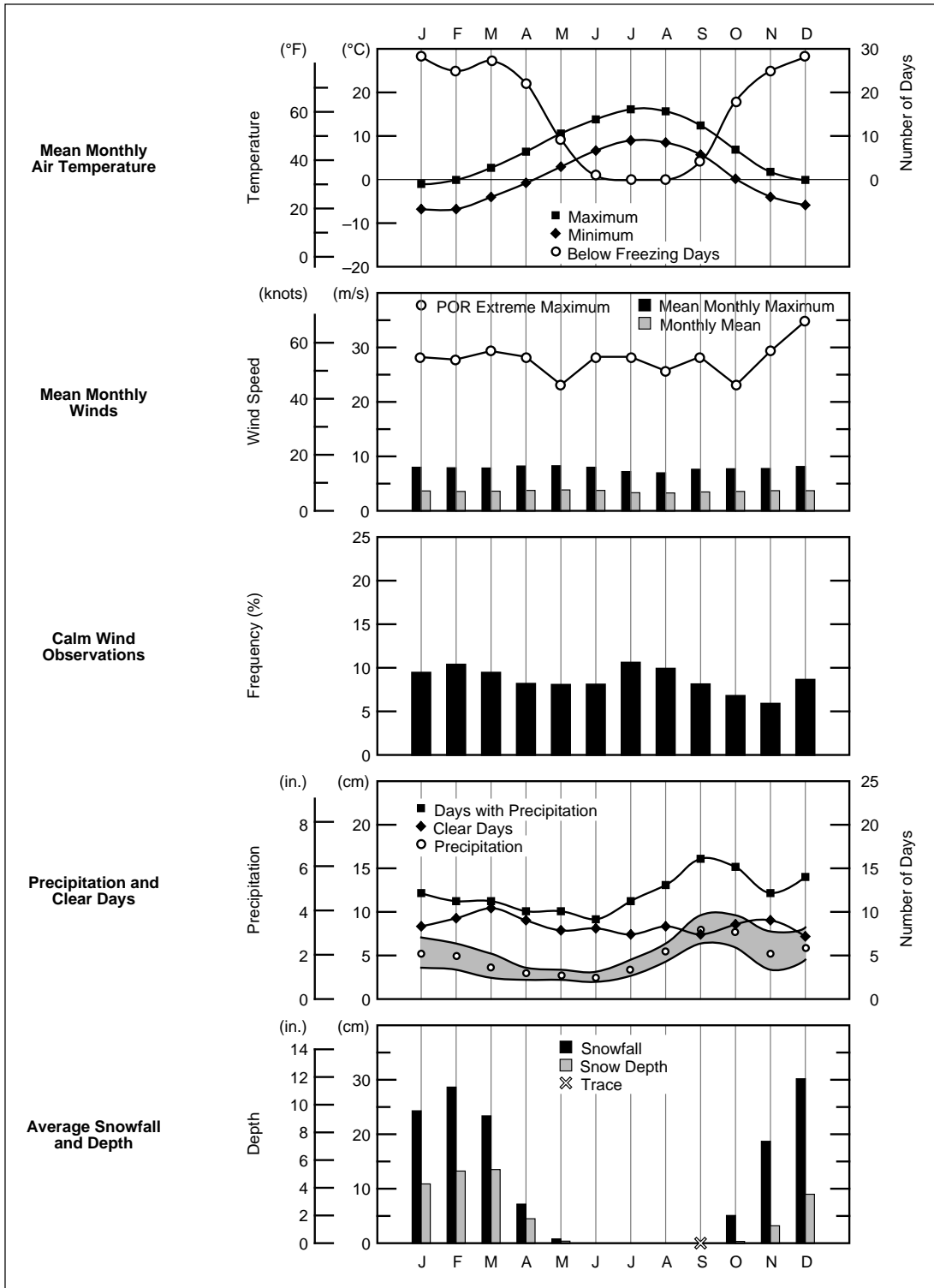


Figure 25. Weather summary for Homer Municipal Airport. The POR is January 1973 to December 1997 except as follows: precipitation (1961–1990) (NCEP 2000), days with measurable precipitation (0.025 cm or more) (1967–1996), clear days (1973–1999), and snowfall and snow depth (1953–1999). The precipitation range is the middle 33% of the data for the 30-year POR; the data points are median values.

6.2.4 Kodiak Airport

The Kodiak weather station is located on the north-eastern end of Kodiak Island, which lies in the western region of the Gulf of Alaska, near the mouth of Cook Inlet. It is 230 km southwest of Homer and 410 km from Anchorage. The Shelikof Strait, approximately 45 km wide, separates it from the mainland. The island is one of several that compose a rugged complex of mountainous terrain approximately 230 km long and 80 km wide. It has numerous ponds, lakes, and interconnecting waterways and a deeply indented shoreline with many deep, narrow bays. The mountaintops range from 600 to 1,500 m with abrupt changes in elevation. The weather station is located on the U.S. Coast Guard Base Kodiak, near the mouth of Womens Bay, an inlet extending westward from Chiniak Bay (NCDC 2000c).

The climate is characteristically maritime, in which air temperature is primarily influenced by the temperature of the surrounding ocean waters. Seasonal and daily temperature swings are diminished. The mean air temperature closely follows the sea surface temperature, rising slightly above it during the warmest month, August, but falling below it again in September. Summer high temperatures average around 16°C, and lows are near 10°C during July and August (Fig. 26). The highest temperature recorded there from 1973 to 1997 was 28°C. Winds at Kodiak are relatively strong throughout the year but diminish somewhat during the summer months (Fig. 26). Monthly mean and monthly maximum winds during June through August are 7–9 and 14–16 knots, respectively. The highest sustained wind speed during June through August for the POR was 58 knots. Calm winds are rare but are most common in July, when they account for less than 5% of all observations (Fig. 26). As is true for the other Cook Inlet stations, the prevailing wind direction is highly dependent on the season. During late spring and summer, there is a strong eastern component. More than 50% of all May-through-July wind observations are out of the northeast–southeast quadrant (see wind roses in Appendix E). In August the winds begin to shift more to the west and northwest, where they remain for most of the rest of the year. July has the least precipitation. However, monthly precipitation amounts vary widely throughout the year in Kodiak. Figure 26 shows three peak precipitation periods (January, May–June, and September–October). The monthly range in near-normal precipitation is large compared to the other Cook Inlet stations. Figure 27 shows the monthly precipitation amounts for the four stations. The lesser amounts for Anchorage, Kenai, and Homer testify to the shel-

tering effect of the Kenai Peninsula and its mountainous barrier to moist-air inflow from the Gulf.

Autumn arrives in early October, when air temperatures begin falling below the freezing mark and snow falls with increased regularity. On average, only one day in September experiences a below-freezing temperature. In November the mean daily low temperature falls below freezing for the month. Monthly mean and maximum wind speeds increase each month, achieving their highest levels in November [5.7 and 12.9 m/s (11 and 25 knots), respectively, with gust winds excluded]. The mean monthly minimum wind speed at Kodiak averages about 2 m/s (4 knots) the entire year, which is twice the speed as at the other Cook Inlet stations. Precipitation amounts increase in the fall, similar to the other Cook Inlet stations. Precipitation during September and October amounts to 21% of the annual total. Interestingly all stations exhibit a significant drop in total precipitation for the month of November, followed by another increase in December.

The mean monthly maximum temperatures remain above freezing throughout the entire winter, while minimum temperatures average only 2–3°C below freezing. The lowest recorded temperature during the 1973 to 1997 POR was –26°C, which occurred in January. Wind speeds remain near the fall levels throughout the winter. The maximum sustained wind speed for the POR, 72 knots, occurred in February. The extreme maximum wind gust recorded at the Kodiak station was 99 knots in January 1950. Gusts of over 50 knots have occurred during every month but are most likely to occur during the winter. About eight storms per year are accompanied by gusts in excess of 55 knots (NOS 1994). Despite the dip in precipitation amount that occurs in November, 51% of the station's annual total falls during the September–January period. The mean number of days having measurable precipitation in Kodiak is nearly 60% higher than in Anchorage, and most of Kodiak's precipitation is in the form of rain. Kodiak receives more than 3.6 times Anchorage's amount of precipitation, but its mean annual snowfall of 162 cm is only about 3% more than that of Anchorage (Fig. 26). The range in snowfall amount from year to year is highly variable in Kodiak, with an extreme maximum in 1956 of 452.4 cm and an extreme minimum of 40.4 cm in 1945 (NOS 1994).

Springtime is accompanied by decreasing wind speeds and precipitation. The prevailing wind transitions to easterly in May, where it remains throughout the summer. Precipitation amounts decrease steadily during February, March, and April before temporarily increasing in May.

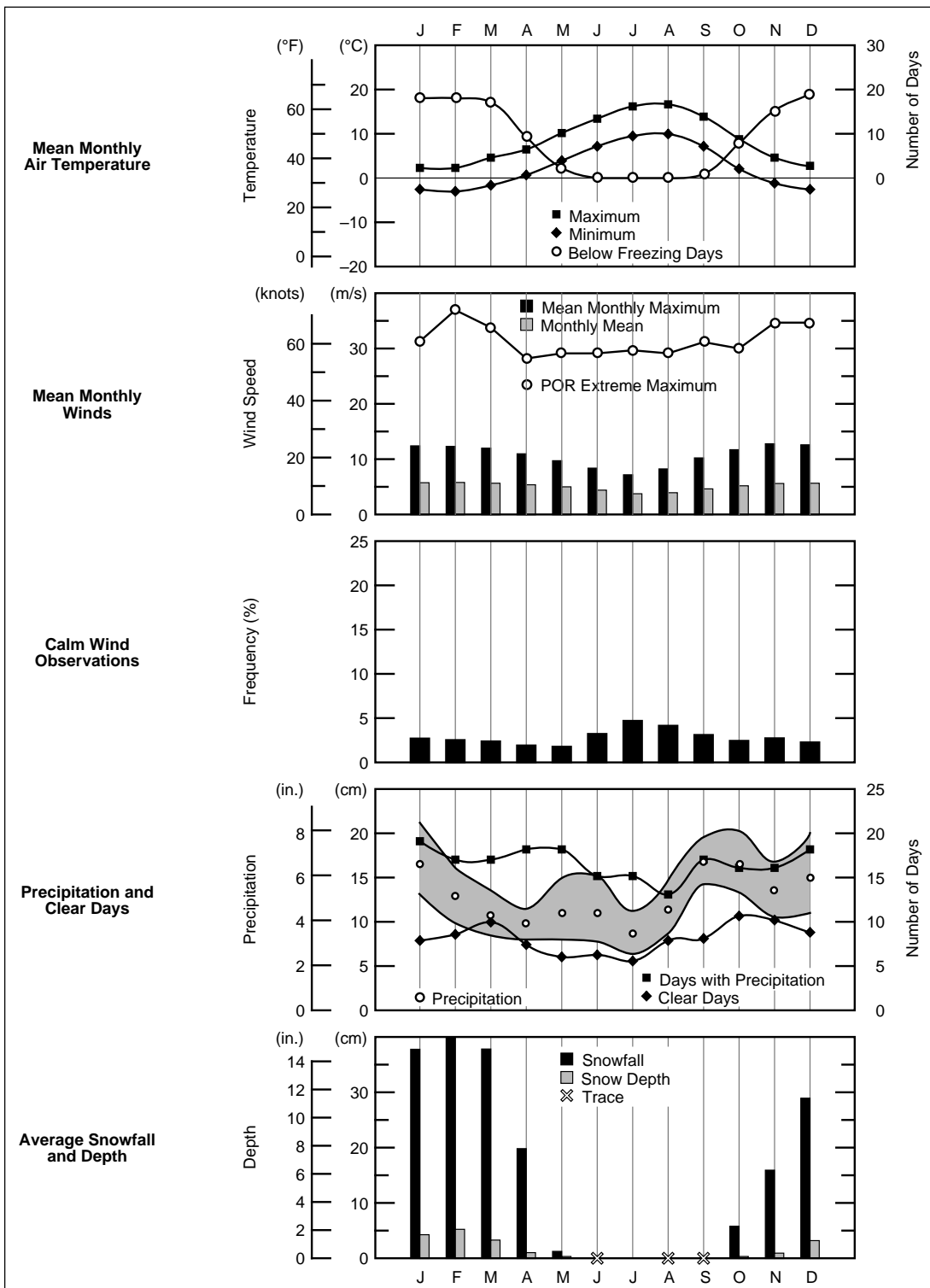


Figure 26. Weather summary for Kodiak Municipal Airport. The POR is January 1973 to December 1997 except as follows: precipitation (1961–1990) (NCEP 2000), days with measurable precipitation (0.025 cm or more) (1967–1996), clear days (1973–1999), and snowfall and snow depth (1953–1999). The precipitation range is the middle 33% of the data for the 30-year POR; the data points are median values.

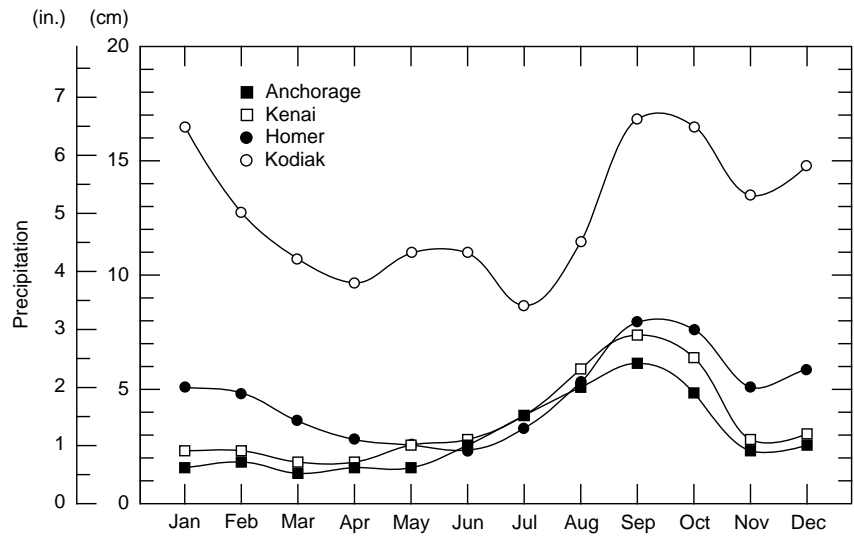


Figure 27. Median monthly precipitation from 1961 to 1990 for four Cook Inlet locations (NCEP 2000).

6.3 Duration of daylight

The duration of daylight is defined as the day's length between sunrise and sunset, and it varies according to location on the earth and time of year. Sunrise and sunset are conventionally considered to occur when the upper edge of the sun is coincident with an unobstructed horizon, under average atmospheric conditions for an observer at sea level. However, at northern latitudes, twilight, when the sun is not far below the horizon, adds significant time of usable light to the period of continuous sunlight. The duration of continuous sunlight plus twilight for a band of northern latitudes is shown in Figure 28. Several representative Alaskan locations are shown for reference. The

figure shows, for example, that Anchorage experiences approximately 13 hours of daylight on March 15 and on October 1.

The times of sunrise and sunset at Kenai for the year 2000 are shown in Table 9, which was generated from a web-based routine that is available at the U.S. Naval Observatory website (USNO 2000). The times shown are accurate to within a few minutes for any other year of interest. A random comparison of dates throughout the 21st century showed that the predicted times of sunrise and sunset agree to within three minutes of those shown for the year 2000. At Kenai the duration of sunlight ranges from about 5.7 hours around December 21 to 19.1 hours around June 21.

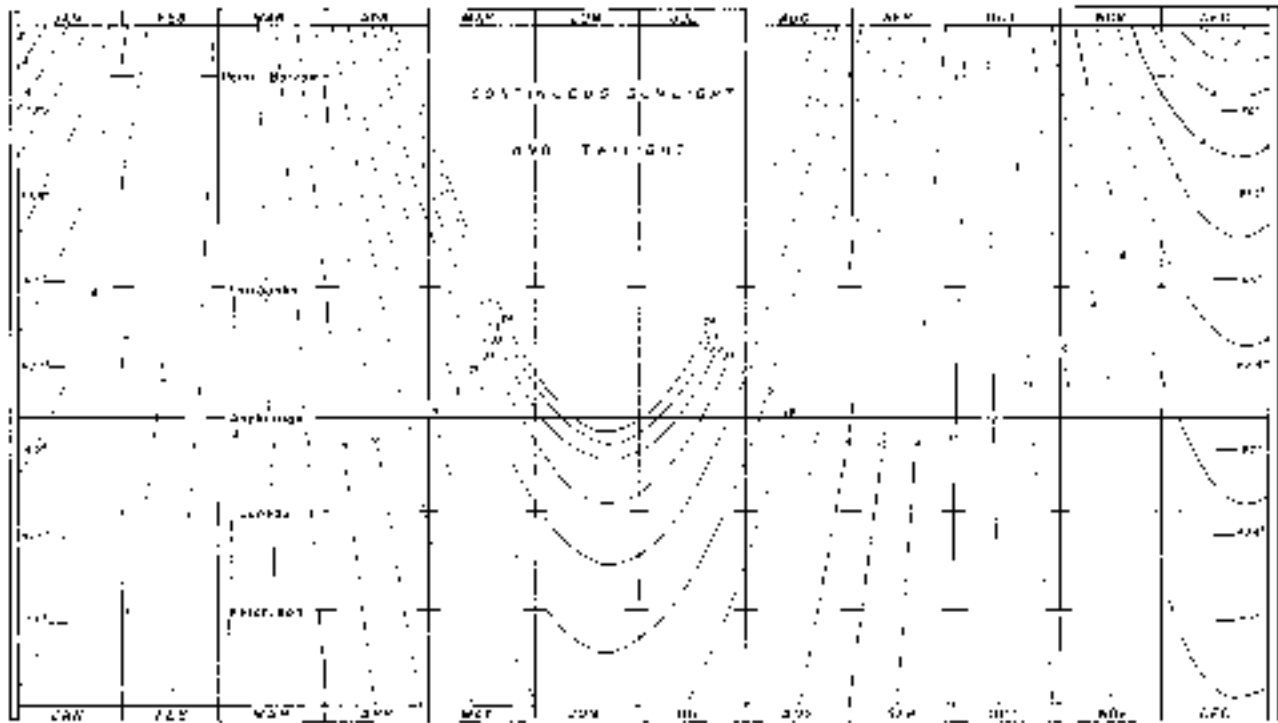


Figure 28. Total length of daylight (combined sunlight and twilight) for Alaska locations. (From Selkregg et al. 1972)

Table 9. Local times of sunrise and sunset at Kenai, Alaska, for the year 2000. The data are from the web site for the Astronomical Applications Department, U.S. Naval Observatory (<http://aa.usno.navy.mil/AA/>).

<i>Day</i>	<i>Jan.</i>		<i>Feb.</i>		<i>Mar.</i>		<i>Apr.</i>		<i>May</i>		<i>June</i>	
	<i>Rise</i>	<i>Set</i>	<i>Rise</i>	<i>Set</i>	<i>Rise</i>	<i>Set</i>	<i>Rise</i>	<i>Set</i>	<i>Rise</i>	<i>Set</i>	<i>Rise</i>	<i>Set</i>
01	1013	1605	0923	1715	0803	1833	0628	1951	0458	2108	0348	2219
02	1012	1606	0920	1718	0800	1836	0624	1954	0456	2110	0346	2221
03	1011	1608	0918	1721	0757	1838	0621	1956	0453	2113	0345	2223
04	1011	1609	0915	1724	0754	1841	0618	1959	0450	2115	0344	2224
05	1010	1611	0913	1726	0751	1843	0615	2001	0447	2118	0342	2226
06	1009	1613	0910	1729	0748	1846	0612	2004	0445	2120	0341	2228
07	1008	1615	0908	1732	0745	1849	0609	2007	0442	2123	0340	2229
08	1007	1617	0905	1734	0742	1851	0606	2009	0439	2125	0339	2230
09	1006	1619	0902	1737	0738	1854	0603	2012	0437	2128	0338	2231
10	1005	1621	0900	1740	0735	1856	0600	2014	0434	2130	0337	2233
11	1003	1623	0857	1743	0732	1859	0557	2017	0432	2133	0337	2234
12	1002	1625	0854	1745	0729	1901	0554	2019	0429	2135	0336	2235
13	1001	1627	0852	1748	0726	1904	0551	2022	0427	2138	0336	2236
14	0959	1630	0849	1751	0723	1906	0548	2024	0424	2140	0335	2236
15	0958	1632	0846	1753	0720	1909	0545	2027	0422	2143	0335	2237
16	0956	1634	0843	1756	0717	1911	0542	2029	0419	2145	0334	2238
17	0954	1637	0840	1759	0714	1914	0539	2032	0417	2148	0334	2238
18	0952	1639	0838	1801	0711	1916	0536	2034	0415	2150	0334	2239
19	0951	1642	0835	1804	0708	1919	0533	2037	0412	2152	0334	2239
20	0949	1644	0832	1807	0705	1921	0530	2039	0410	2155	0334	2239
21	0947	1647	0829	1809	0702	1924	0527	2042	0408	2157	0334	2239
22	0945	1649	0826	1812	0658	1926	0524	2045	0406	2159	0335	2240
23	0943	1652	0823	1815	0655	1929	0521	2047	0404	2201	0335	2239
24	0941	1654	0820	1817	0652	1931	0518	2050	0402	2204	0336	2239
25	0939	1657	0817	1820	0649	1934	0515	2052	0400	2206	0336	2239
26	0936	1659	0814	1823	0646	1936	0512	2055	0358	2208	0337	2239
27	0934	1702	0812	1825	0643	1939	0510	2057	0356	2210	0338	2238
28	0932	1705	0809	1828	0640	1941	0507	2100	0354	2212	0339	2238
29	0930	1707	0806	1831	0637	1944	0504	2103	0353	2214	0340	2237
30	0927	1710			0634	1946	0501	2105	0351	2216	0341	2236
31	0925	1713			0631	1949			0349	2218		

Times are given for Alaska Standard time; add one hour for daylight time, if and when in use.

Table 9 (cont'd).

<i>July</i>		<i>Aug.</i>		<i>Sept.</i>		<i>Oct.</i>		<i>Nov.</i>		<i>Dec.</i>	
<i>Rise</i>	<i>Set</i>	<i>Rise</i>	<i>Set</i>	<i>Rise</i>	<i>Set</i>	<i>Rise</i>	<i>Set</i>	<i>Rise</i>	<i>Set</i>	<i>Rise</i>	<i>Set</i>
0342	2236	0444	2137	0600	2008	0712	1835	0831	1705	0946	1602
0343	2235	0446	2135	0602	2005	0715	1832	0834	1702	0948	1601
0344	2234	0449	2132	0605	2002	0717	1829	0837	1700	0950	1600
0346	2233	0451	2129	0607	1959	0720	1826	0839	1657	0952	1559
0347	2232	0453	2127	0610	1956	0722	1823	0842	1655	0954	1558
0349	2230	0456	2124	0612	1953	0725	1820	0845	1652	0956	1557
0350	2229	0458	2121	0615	1950	0727	1817	0847	1649	0957	1556
0352	2228	0501	2119	0617	1946	0730	1814	0850	1647	0959	1555
0353	2226	0503	2116	0619	1943	0732	1811	0853	1645	1001	1555
0355	2225	0506	2113	0622	1940	0735	1808	0855	1642	1002	1554
0357	2223	0508	2110	0624	1937	0737	1805	0858	1640	1003	1554
0359	2221	0511	2107	0627	1934	0740	1802	0900	1637	1005	1553
0401	2220	0513	2105	0629	1931	0742	1759	0903	1635	1006	1553
0403	2218	0516	2102	0631	1928	0745	1756	0906	1633	1007	1553
0405	2216	0518	2059	0634	1925	0747	1753	0908	1631	1008	1553
0407	2214	0521	2056	0636	1922	0750	1750	0911	1628	1009	1553
0409	2212	0523	2053	0639	1918	0752	1747	0913	1626	1010	1553
0411	2210	0526	2050	0641	1915	0755	1744	0916	1624	1011	1553
0413	2208	0528	2047	0643	1912	0758	1741	0918	1622	1012	1553
0415	2206	0531	2044	0646	1909	0800	1738	0921	1620	1012	1554
0418	2204	0533	2041	0648	1906	0803	1735	0923	1618	1013	1554
0420	2202	0536	2038	0651	1903	0805	1733	0926	1616	1013	1555
0422	2159	0538	2035	0653	1900	0808	1730	0928	1615	1014	1556
0424	2157	0541	2032	0656	1857	0810	1727	0931	1613	1014	1556
0427	2155	0543	2029	0658	1854	0813	1724	0933	1611	1014	1557
0429	2152	0545	2026	0700	1851	0816	1721	0935	1609	1014	1558
0432	2150	0548	2023	0703	1848	0818	1718	0938	1608	1014	1559
0434	2147	0550	2020	0705	1844	0821	1716	0940	1606	1014	1600
0436	2145	0553	2017	0708	1841	0824	1713	0942	1605	1014	1602
0439	2142	0555	2014	0710	1838	0826	1710	0944	1604	1013	1603
0441	2140	0558	2011			0829	1708			1013	1604

7 LITERATURE CITED

- ACRC** (1997a) Alaska monthly precipitation, cloudiness, relative humidity, wind. Alaska climatology page. <http://climate.gi.alaska.edu/AKCityClimo/akclimo.html> (revised 22 Sep.1997), Alaska Climate Research Center, University of Alaska Fairbanks.
- ACRC** (1997b) Alaska monthly temperature record. Alaska climatology page. <http://climate.gi.alaska.edu/AKCityClimo/akclimo1.html> (revised 22 Sep.1997), Alaska Climate Research Center, University of Alaska Fairbanks.
- ADEC** (1999) Situation Report #4. Alaska Department of Environmental Conservation, Anchorage.
- AEIDC** (1974) Alaska regional profiles, southcentral region. Arctic Environmental Information and Data Center, University of Alaska Anchorage.
- API** (1988) RP 2N, Recommended practice for planning, design, and constructing fixed offshore structures in ice environments. American Petroleum Institute, Dallas.
- Associated Press** (1999) East shore ice halts Kenai-area shipping. *Anchorage (Alaska) Daily News*, 9 February 1999, p. B1.
- Bhat, S.U., and G.F.N. Cox** (1995) Ice loads on multi-legged structures in Cook Inlet. In *Proceedings, 13th International Conference on Port and Ocean Engineering under Arctic Conditions*, Murmansk, Russia, Aug. 15–18, 1995, vol. 4, p. 51–61.
- Bilello, M.A.** (1980) Maximum thickness and subsequent decay of lake, river, and fast sea ice in Canada and Alaska. CRREL Report 80-6, U.S. Army Cold Regions Research and Engineering Laboratory, Hanover, New Hampshire.
- Blenkarn, K.A.** (1970) Measurement and analysis of ice forces on Cook Inlet structures. In *Proceedings of the Offshore Technology Conference*, 22–24 April 1970, Dallas, Texas. Offshore Technology Conference, Richardson, Texas.
- Bowditch, N.** (1979) *Marine Weather*. New York: Arco Publishing, Inc.
- Brower, W.A., Jr., R.G. Baldwin, C.N. Williams, Jr., J.L. Wise, and L.D. Leslie** (1988) *Climatic Atlas of the Outer Continental Shelf Waters and Coastal Regions of Alaska; Vol. I. Gulf of Alaska, Vol. II. Bering Sea, Vol. III. Chukchi-Beaufort Sea*. Anchorage, Alaska: Arctic Environmental Information and Data Center.
- Eaton, R.B., III** (1980) Sea ice conditions in the Cook Inlet, Alaska during the 1977-78 winter. NOAA Technical Memorandum NWS AR-28, U.S. National Oceanic and Atmospheric Administration, National Weather Service, Anchorage, Alaska.
- Gatto, L.W.** (1976) Baseline data on the oceanography of Cook Inlet, Alaska. CRREL Report 76-25, U.S. Army Cold Regions Research and Engineering Laboratory, Hanover, N.H.
- Hutcheon, R.J.** (1972a) Sea ice conditions in the Cook Inlet, Alaska during the 1969-1970 winter. NOAA Technical Memorandum AR-6, U.S. National Oceanic and Atmospheric Administration, National Weather Service, Anchorage, Alaska.
- Hutcheon, R.J.** (1972b) Sea ice conditions in the Cook Inlet, Alaska during the 1970-1971 winter. NOAA Technical Memorandum AR-7, U.S. National Oceanic and Atmospheric Administration, National Weather Service, Anchorage, Alaska.
- Hutcheon, R.J.** (1973) Sea ice conditions in the Cook Inlet, Alaska during the 1971-72 winter. NOAA Technical Memorandum AR-8, U.S. National Oceanic and Atmospheric Administration, National Weather Service, Anchorage, Alaska.
- International Marine** (1996) *Tide Tables 1996: West Coast of North and South America including the Hawaiian Islands*. Camden, Maine: International Marine/Ragged Mountain Press.

- Kizzia, T.** (1990) Tankers fight Cook Inlet ice, Oil loading now takes days. *Anchorage (Alaska) Daily News*, 9 February 1990, p. B1.
- LaBelle, J.C., J.L. Wise, R.P. Voelker, R.H. Schulze, and G.M. Wohl** (1983) *Alaska Marine Ice Atlas*. University of Alaska, Anchorage: Arctic Environmental Information and Data Center.
- Little, J.** (1999) Ships stalled by ice. *Anchorage (Alaska) Daily News*, 11 February 1999, p. B1.
- Little, J.** (2000a) Cook Inlet ice disables freighter, Prompts Coast Guard to toughen rules. *Anchorage (Alaska) Daily News*, 15 January 2000, p. B1.
- Little, J.** (2000b) Inlet ice shuts 2 Nikiski docks. *Anchorage (Alaska) Daily News*, 21 January 2000, p. B1.
- Muench, R.D., H.O. Mofjeld, and R.L. Charnell** (1978) Oceanographic conditions in lower Cook Inlet: Spring and summer 1973. *Journal of Geophysical Research*, **83** (C10): 5090–5098.
- Murphy, R.S., R.F. Carlson, D. Nyquist, and R. Britch** (1972) Effect of waste discharges into a silt laden estuary, A case study of Cook Inlet, Alaska. Report IWR-26, Institute of Water Resources, University of Alaska Fairbanks.
- NCDC** (2000a) Anchorage International Airport. Locate weather observation station record. <http://www4.ncdc.noaa.gov/cgi-win/wwcgi.dll?wwDI~StnSrch~StnID~20022040> (revised 20 Apr. 2000), National Climatic Data Center, Asheville, N.C.
- NCDC** (2000b) Homer Airport. Locate weather observation station record. <http://www4.ncdc.noaa.gov/cgi-win/wwcgi.dll?wwDI~StnSrch~StnID~20021939> (revised 20 Apr. 2000), National Climatic Data Center, Asheville, N.C.
- NCDC** (2000c) Kodiak Airport. Locate weather observation station record. <http://www4.ncdc.noaa.gov/cgi-win/wwcgi.dll?wwDI~StnSrch~StnID~20021863> (revised 20 Apr. 2000), National Climatic Data Center, Asheville, N.C.
- NCEP** (2000) Climatological data tables for [each month]. CPC: Monthly Outlook – Climatological Monthly Data. http://www.cpc.noaa.gov/products/predictions/monthly_climate/data/ (downloaded 22 Mar 2000), Climate Prediction Center, National Centers for Environmental Prediction, National Oceanic and Atmospheric Administration, Washington, D.C.
- Nelson, W.G.** (1995) Sea ice formation in Cook Inlet Alaska: A high energy environment. In *Proceedings, 14th International Conference on Offshore Mechanics and Arctic Engineering (OMAE)*, Copenhagen, Denmark, June 18–22, 1995 (W.A. Nixon, D.S. Sodhi, N.K. Sinha, and F.T. Christensen, Ed.). New York: American Society of Mechanical Engineers, vol. 4, p. 53–59.
- NIC** (2000) West Arctic Web Page: Cook Inlet Region. <http://www.natice.noaa.gov/>. National Oceanic and Atmospheric Administration, National Ice Center, Washington, D.C.
- NOS** (1994) *United States Coast Pilot. Pacific and Arctic Coasts Alaska: Cape Spencer to Beaufort Sea*. 16th Ed., National Oceanic and Atmospheric Administration, National Ocean Service, Silver Spring, Maryland.
- NOS** (1997) *United States Alaska – South Coast: Cook Inlet Southern Part*. Chart 16640, 23rd Ed., National Oceanic and Atmospheric Administration, National Ocean Service, Silver Spring, Maryland.
- NWS** (2000) Cook Inlet ice analysis. Sea surface temperatures and sea ice analysis. <http://www.alaska.net/~nwsfoanc/> (downloaded 20 Apr. 2000), National Weather Service, Forecast Office, Anchorage.
- Page, R.** (1997) Alaska Sea Ice/SST Desk: Providing products in a data sparse area. In *Proceedings, 13th International Conference on IIPS for Meteorology, Oceanography, and Hydrology*, 2–7 Feb. 1997, Longbeach, California, American Meteorological Society, p. 373–376.
- Pearce, B., D. Jones, and H. McIlvane** (1999) An overview of CIOISM 2.0 – The Cook Inlet oil spill model. In *Proceedings, Cook Inlet Oceanography Workshop, Kenai, Alaska*, 9 November 1999 (M.A. Johnson and S.R. Okkonen, ed.). Coastal Marine Institute, University of Alaska Fairbanks, p. 59–69.
- Poole, F.W.** (1980) Sea ice conditions in Cook Inlet, Alaska, during the 1976-1977 winter. NOAA Technical Memorandum NWS AR-27, U.S. National Oceanic and Atmospheric Administration, National Weather Service, Anchorage, Alaska.
- Poole, F.W.** (1981a) Sea ice conditions in Cook Inlet, Alaska, during the 1978-1979 winter. NOAA Technical Memorandum NWS AR-30, U.S. National Oceanic and Atmospheric Administration, National Weather Service, Anchorage, Alaska.
- Poole, F.W.** (1981b) Sea ice conditions in Cook Inlet, Alaska during the 1979-1980 winter. NOAA Technical Memorandum NWS AR-32, U.S. National Oceanic and Atmospheric Administration, National Weather Service, Anchorage, Alaska.
- Poole, F.W., and G.L. Hufford** (1982) Meteorological and oceanographic factors affecting sea ice in Cook Inlet. *Journal of Geophysical Research*, **87** (C3): 2061–2070.
- Raney, D.C.** (1993) Numerical modeling of extreme tidal conditions in Upper Cook Inlet, Alaska. BER Report Number 587-183, Bureau of Engineering Research, University of Alabama, Tuscaloosa.
- Rappeport, M.L.** (1982) Analysis of oceanographic and meteorological conditions for central lower Cook

- Inlet, Alaska. U.S. Geological Survey, vol. 82, no. 128.
- Sanderson, T.J.O.** (1988) Measurements on narrow structures. In *Ice Mechanics, Risk to Offshore Structures*. London: Graham and Trotman, p. 110–112.
- Schulz, R.** (1977a) Sea ice conditions in Cook Inlet, Alaska during the 1972-73 winter. NOAA Technical Memorandum NWS AR-17, U.S. National Oceanic and Atmospheric Administration, National Weather Service, Anchorage, Alaska.
- Schulz, R.** (1977b) Sea ice conditions in Cook Inlet, Alaska during the 1973-74 winter. NOAA Technical Memorandum NWS AR-18, U.S. National Oceanic and Atmospheric Administration, National Weather Service, Anchorage, Alaska.
- Schulz, R.** (1977c) Sea ice conditions in Cook Inlet, Alaska during the 1974-75 winter. NOAA Technical Memorandum NWS AR-19, U.S. National Oceanic and Atmospheric Administration, National Weather Service, Anchorage, Alaska.
- Schulz, R.** (1978). Sea ice conditions in Cook Inlet, Alaska during the 1975-76 winter. NOAA Technical Memorandum NWS AR-20, U.S. National Oceanic and Atmospheric Administration, National Weather Service, Anchorage, Alaska.
- Selkregg, L.L., E.H. Buck, R.T. Buffler, O.E. Coté, C.D. Evans, and S.G. Fisk (Ed.)** (1972) *Environmental Atlas of the Greater Anchorage Area Borough, Alaska*. Anchorage, Alaska: Resource and Science Services, Arctic Environmental Information and Data Center, University of Alaska.
- Siple, P.A., and C.F. Passel** (1945) Measurements of dry atmospheric cooling in subfreezing temperatures. *Proceedings, American Philosophical Society*, **89**: 177–199.
- Smith, O.** (2000) Formation and decay of stamukhas, Cook Inlet, Alaska. *Proceedings, 15th International Symposium on Ice*, Gdansk, Poland, 28 August – 1 September 2000. Institute of Hydroengineering, Gdansk, Poland.
- Smith, O.P.** (unpublished) Comparison of 1996-1997 winter navigation conditions on Knik Arm, Alaska, to previous years' climate. Internal report, U.S. Army Cold Regions Research and Engineering Laboratory, Hanover, New Hampshire.
- Untersteiner, N.** (1986) *The Geophysics of Sea Ice*. New York: Plenum Press, p. 422–428.
- USACE** (1993) Deep draft navigation reconnaissance report, Cook Inlet, Alaska. U.S. Army Corps of Engineers Alaska District. Anchorage, Alaska.
- USCB** (1999) Population estimates for places: Annual time series, July 1, 1990 to July 1, 1998. Census Bureau: Annual Time Series of Population Estimates, 1991 to 1998, and 1990 Census Population for Places. http://www.census.gov/population/estimates/metro-city/scts/SC98T_AK-DR.txt (revised 14 Dec. 1999). Population Division, U.S. Census Bureau, Washington, D.C.
- USCG** (1991) Waterway analysis for Cook Inlet West/North. 17th Coast Guard District, Juneau, Alaska.
- USNO** (2000) Kenai, Alaska rise and set for the sun for 2000. Sun or Moon Rise/Set Table for One Year. <http://aa.usno.navy.mil/AA/> (revised 22 Feb. 2000), U.S. Naval Observatory, Astronomical Applications Dept., Washington, D.C.
- Utt, M.E., and B.E. Turner** (1992) Cook Inlet ice loads calculated using historical data and probabilistic methods. In *Proceedings, Second International Offshore and Polar Engineering Conference*, San Francisco, June 14–19, 1992 (M.S. Triantafyllou, J.S. Chung, K. Karal, and A.L. Tunik, ed.). Golden, Colorado: International Society of Offshore and Polar Engineers, p. 677–680.
- Visser, R.C.** (1992) A retrospective of platform development in Cook Inlet, Alaska. *Journal of Petroleum Technology*, **44**(2): 146–203.
- Weingartner, T.J.** (1992) Circulation studies in Shelikof Strait, Cook Inlet, and the Gulf of Alaska. In *Proceedings, Fourth Alaska Outer Continental Shelf (AOCS) Region Information Transfer Meeting*, Anchorage, Alaska, U.S. Minerals Management Service, p. 41–51.
- Wohlforth, C.** (1990) Oil shipments may be stopped for heavy ice, panel chief says. *Anchorage (Alaska) Daily News*, 19 December 1990, p. B1.
- WMO** (1970) WMO sea-ice nomenclature. WMO/OMM/BMO No. 259. TP. 145, Geneva, Switzerland.
- Zubov, N.N.** (1945) Arctic ice. Northern Sea Route Administration, Moscow, U.S.S.R. Translated by the U.S. Naval Oceanographic Office.

